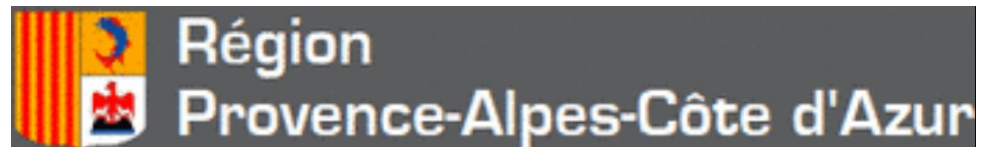


Current issues in coherence for small laser sources

G.L. Lippi

Institut Non Linéaire de Nice
Université de Nice-Sophia Antipolis
and
UMR 7335 CNRS

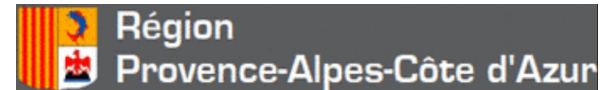
with the support of :



Coworkers

At the INLN

Experiments Tao Wang (Ph.D. Student)



B. Benzimoun (Intern, Univ. Clermont-Ferrand)

At CNR (Italy)

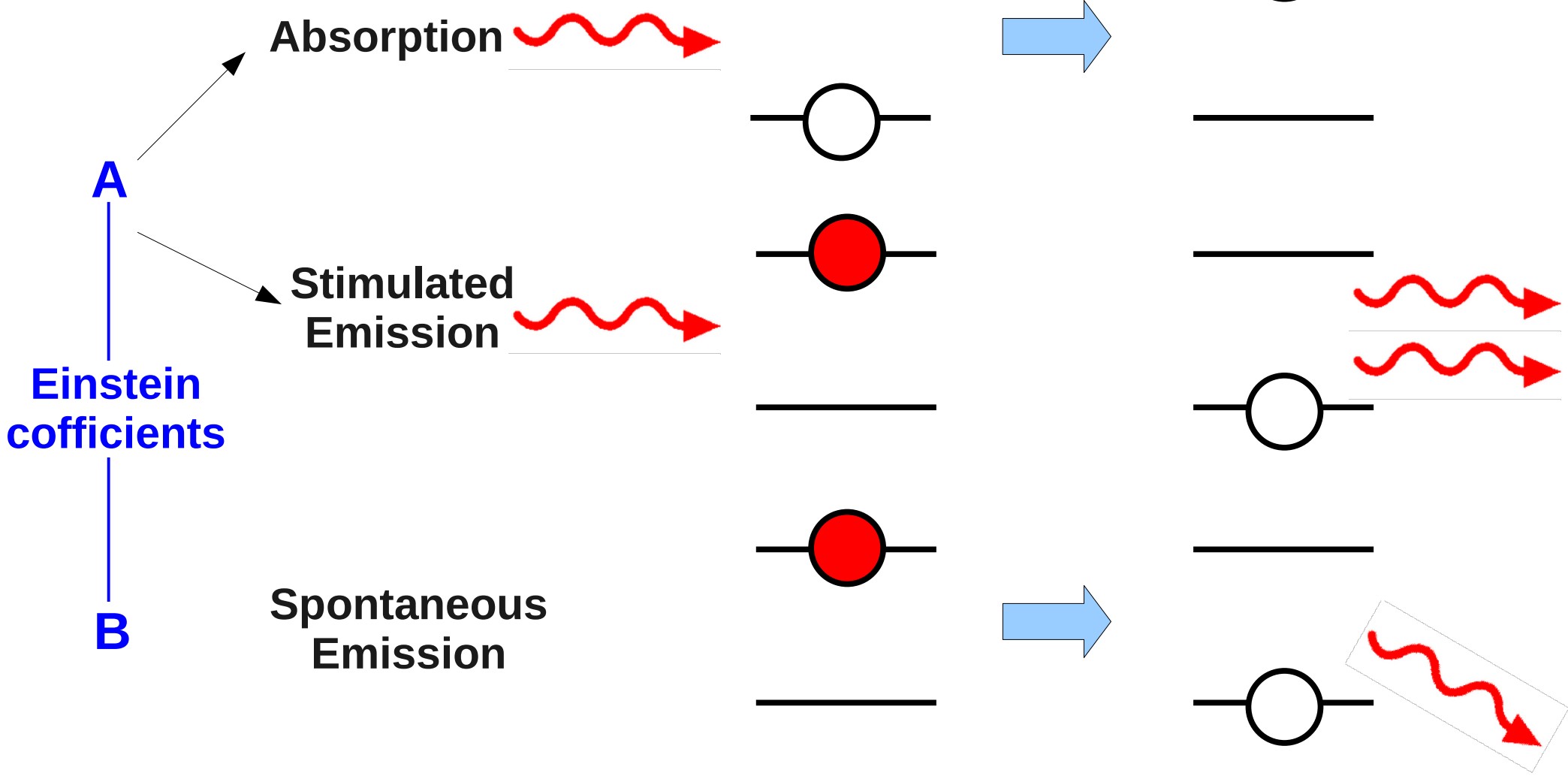
Numerics G.P. Puccioni – Firenze
(Italy)



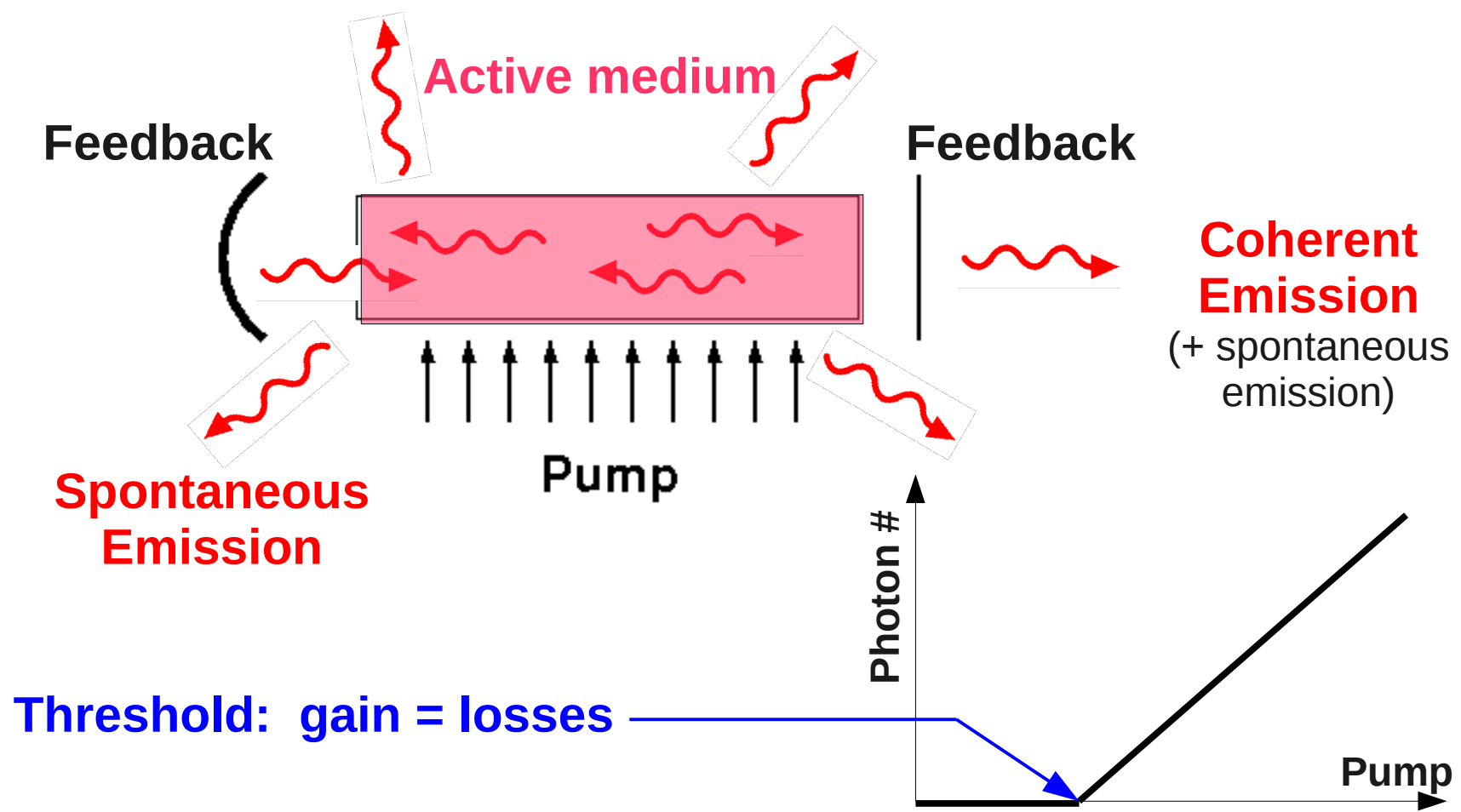
Outline of talk

- 0. General Introduction and Overview of the Problem**
- I. Coherence in Macroscopic Lasers**
- II. Coherence in Micro- and Nanolasers**
- III. Statistical Mixture of Thermal and Coherent light**
- IV. Oscillations in Coherence Function**
- V. Additional Remarks**

Brief reminder

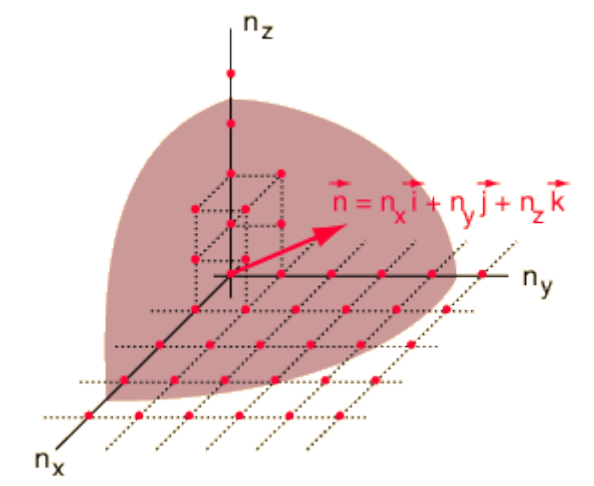
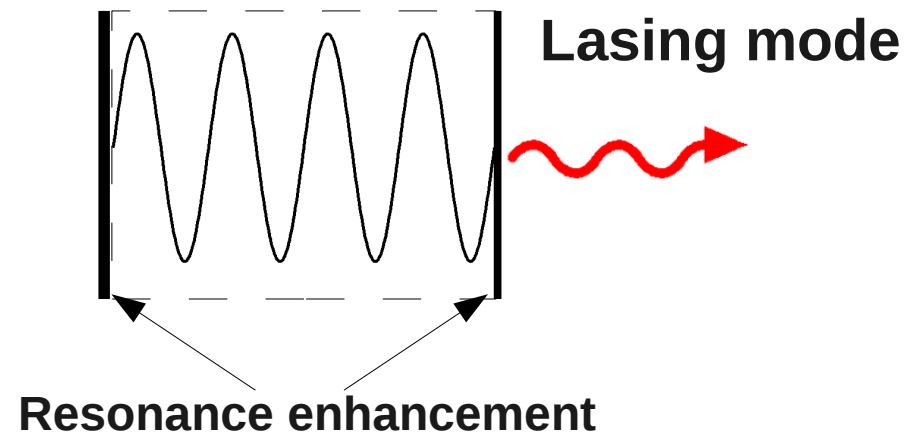


Brief reminder

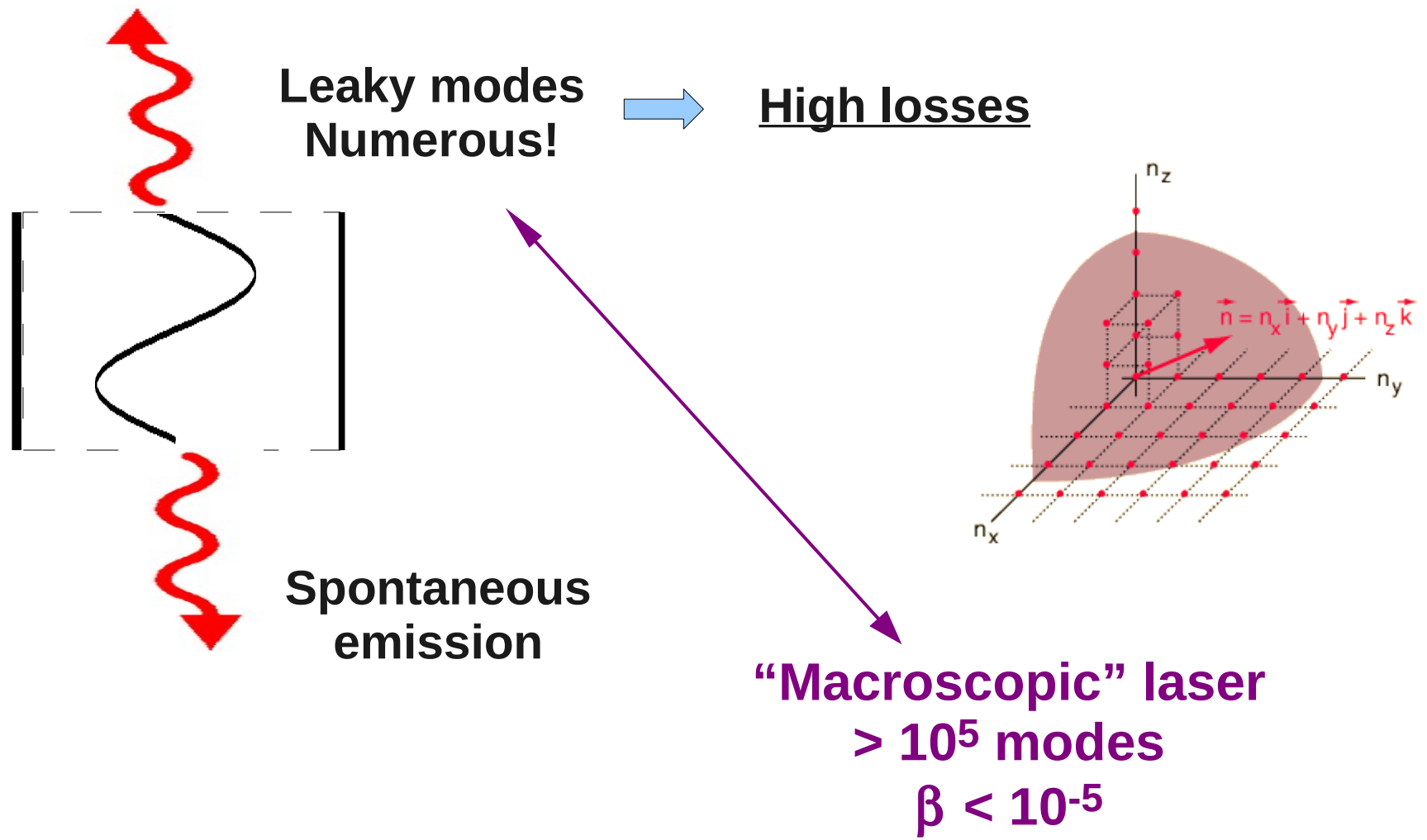


Threshold: gain = losses

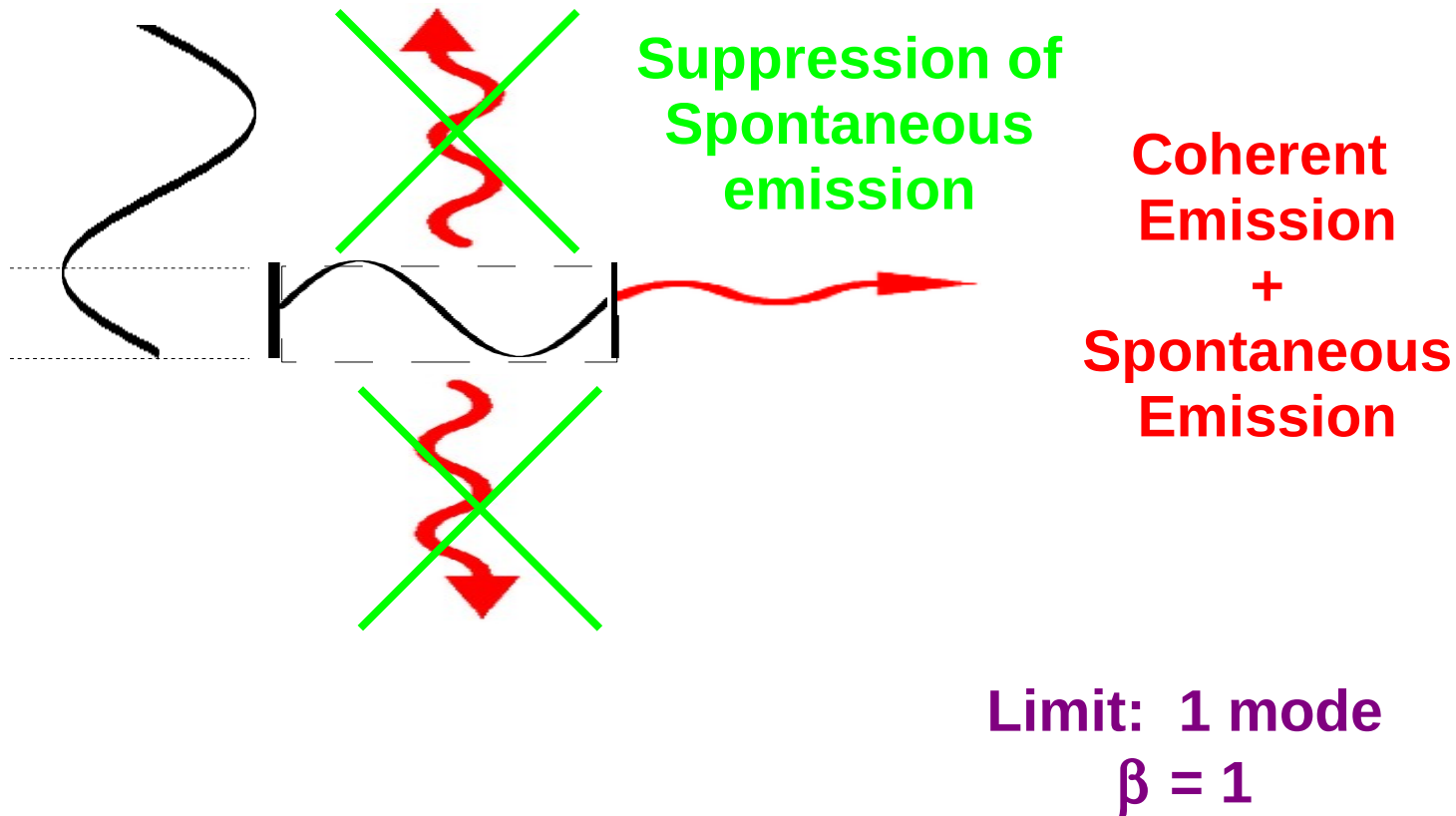
Cavity modes



Cavity modes



Nanolaser



I. Coherence in Macroscopic Lasers

Experiments (and theory)

He-Ne $\lambda = 6328 \text{ \AA}$

Cavity volume $\sim 1 \text{ cm}^3$

$\beta < 10^{-8}$

Photocount Distributions and Field Statistics.

F. T. ARECCHI

CISE Laboratories - Segrate (Milano)
Istituto di Fisica dell'Università - Milano

Thermal light photocount statistics:
Laser light photocount statistics:
Superposition of thermal and laser light:

G
L
S

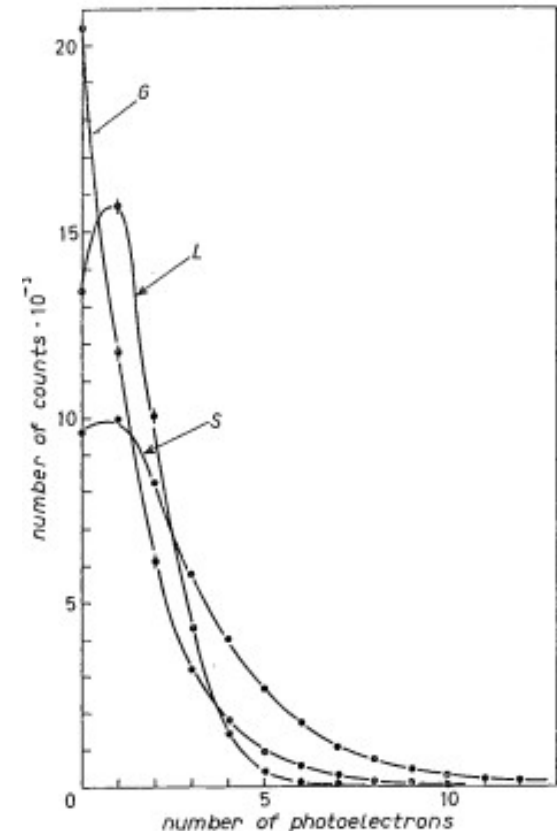


Fig. 2. - Photocount distributions of a Gaussian field, a laser field, and a field made by the superposition of the two (nonlinear method); *G*, gaussian light; *L*, laser light; and *S*, superposed light. The three curves are not normalized.

Photocount Distributions and Field Statistics.

F. T. ARECCHI

CISE Laboratories - Segrate (Milano)
Istituto di Fisica dell'Università - Milano

Evolution of the
statistical photon
mixture

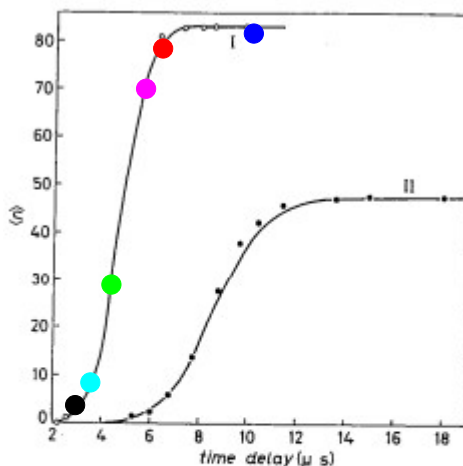


Fig. 23. - Evolution of the mean value $\langle n \rangle$ of the statistical distribution $p(n, T, \tau)$. The solid lines represent the theoretical curves which best fit the experimental points (o, •). The experimental points related to curve I have been obtained by the statistical distributions of Fig. 22.

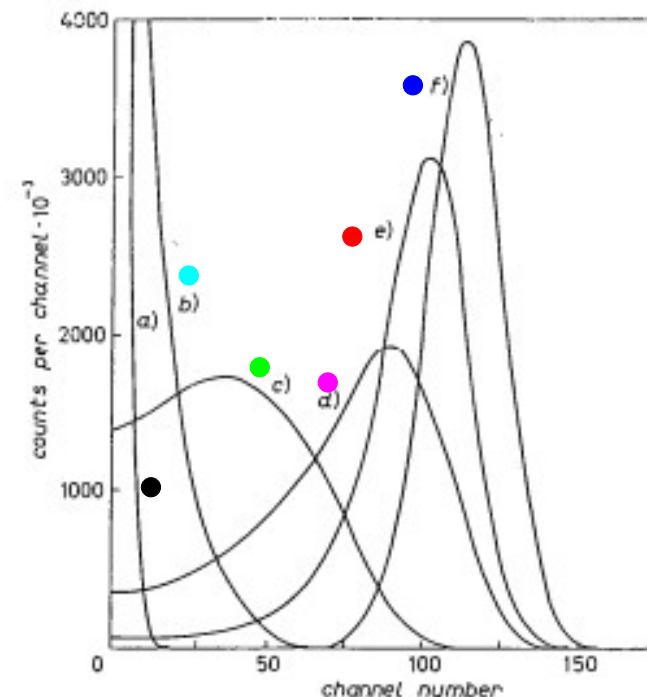


Fig. 22. - Experimental statistical distributions with different time delays obtained on a laser transient. The solid lines connect the experimental points which are not shown to make clearer the figure. All distributions are normalized to the same area a) 2.6 μs ; b) 3.7 μs ; c) 4.3 μs ; d) 5 μs ; e) 5.6 μs ; f) 8.8 μs .

Photocount Distributions and Field Statistics.

F. T. ARECCHI

CISE Laboratories - Segrate (Milano)
Istituto di Fisica dell'Università - Milano

$$(6.28) \quad H_2 = \frac{\langle n(n-1) \rangle}{\langle n \rangle^2} - 1,$$

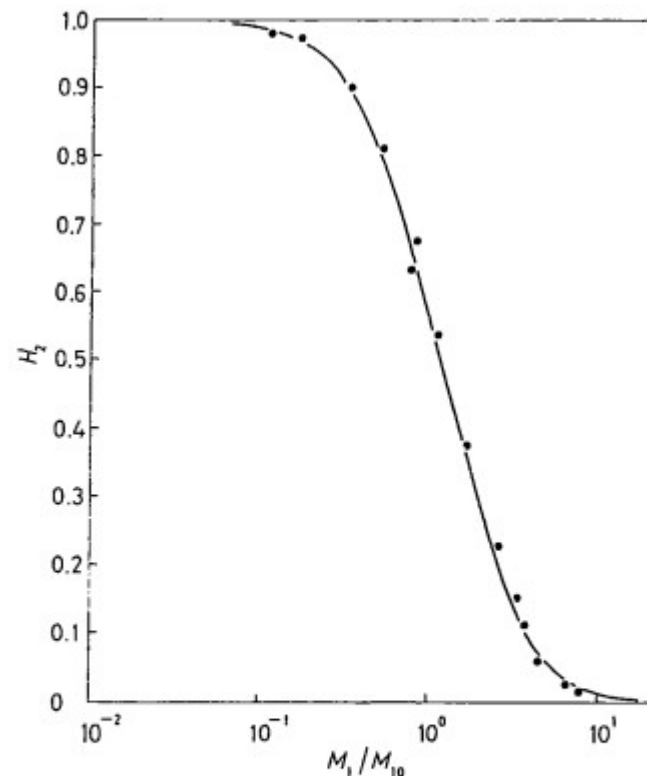


Fig. 17. - Measured and theoretical values of the reduced second-order factorial moment H_2 as a function of the normalized intensity M_1/M_{10} in the threshold region. — Theory; • experimental point.

Photocount Distributions and Field Statistics.

F. T. ARECCHI

CISE Laboratories - Segrate (Milano)
Istituto di Fisica dell'Università - Milano

$$(6.29) \quad H_3 = \frac{\langle n(n-1)(n-2) \rangle}{\langle n \rangle^3} - 1,$$

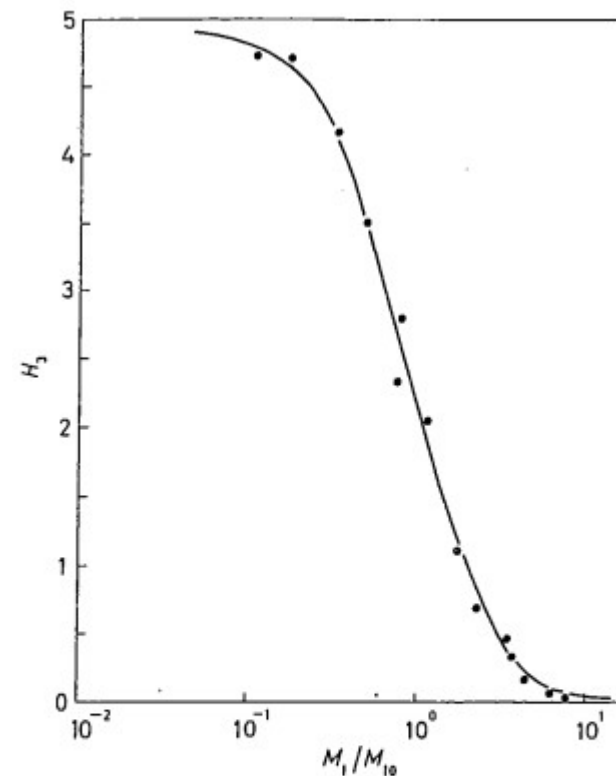


Fig. 18. - Measured and theoretical values of the reduced third-order factorial moment H_3 as a function of the normalized intensity M_1/M_{10} in the threshold region. — Theory, • experimental point.

II. Coherence in Micro- and Nanolasers

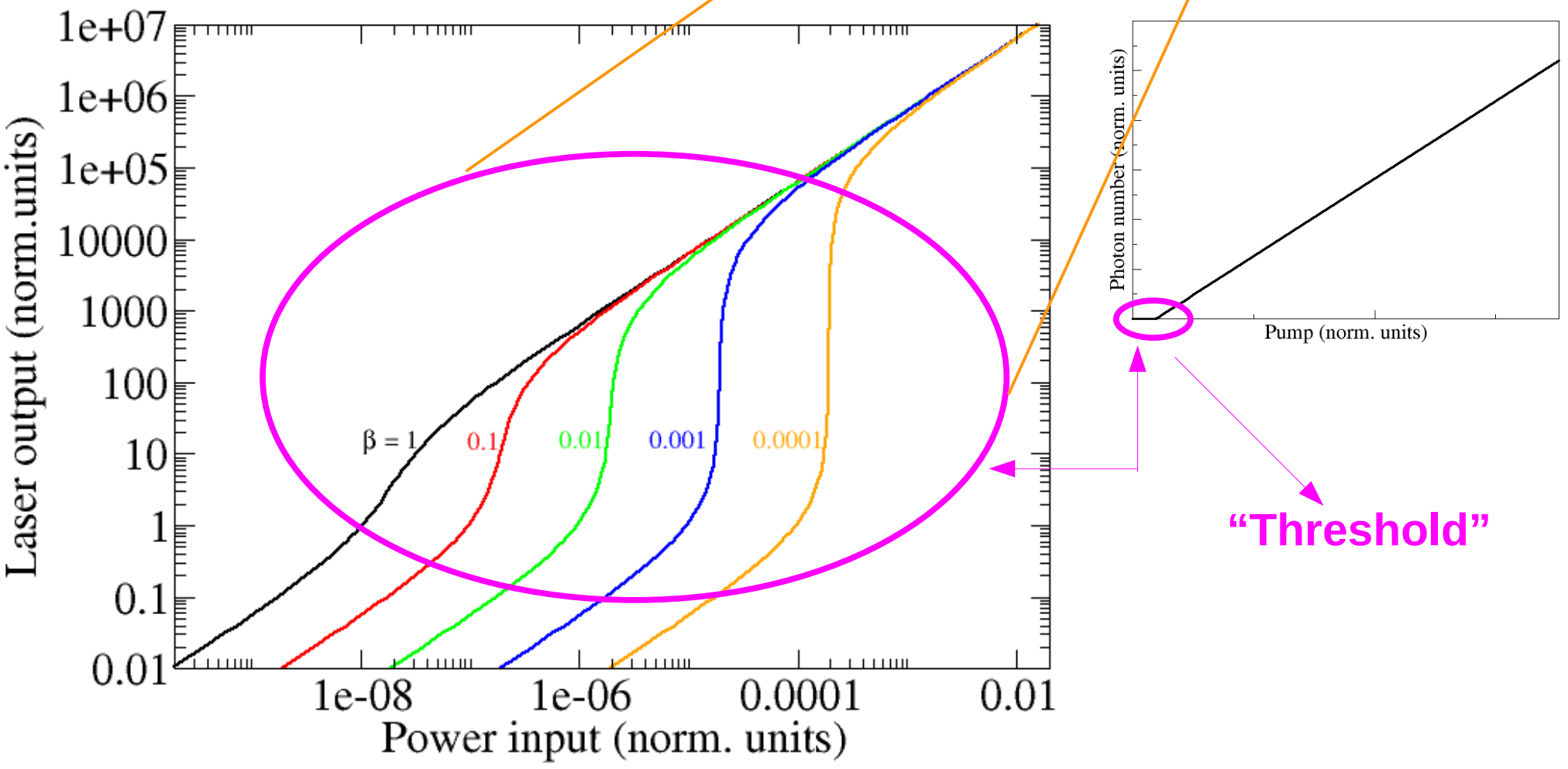
Experiments and theory

$$0.8 \mu\text{m} < \lambda < 1.5 \mu\text{m}$$

$$\text{Cavity volume} < 10 \mu\text{m}^3$$
$$\beta > 10^{-4}$$

Threshold representation

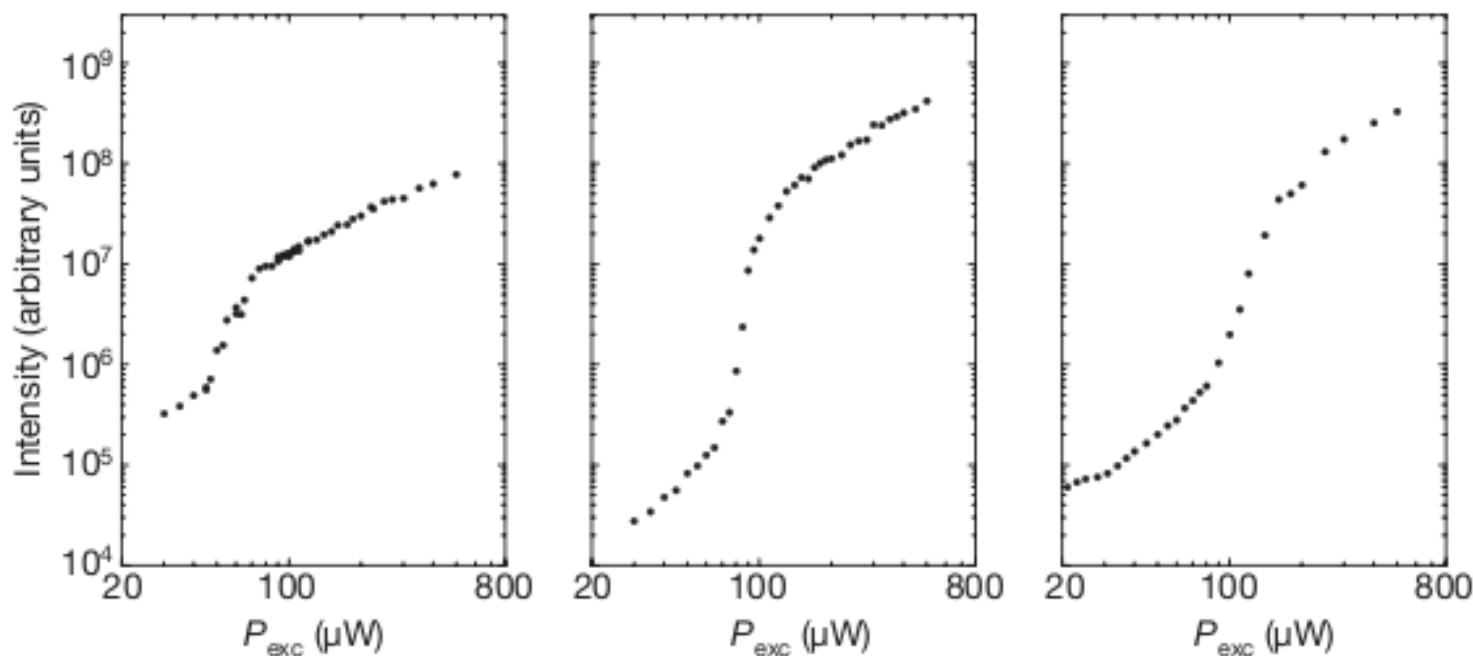
Coherence?



Vol 460 | 9 July 2009 | doi:10.1038/nature08126

Direct observation of correlations between individual photon emission events of a microcavity laser

J. Wiersig^{1†}, C. Gies¹, F. Jahnke¹, M. Aßmann², T. Berstermann², M. Bayer², C. Kistner³, S. Reitzenstein³, C. Schneider³, S. Höfling³, A. Forchel³, C. Kruse¹, J. Kalden¹ & D. Hommel¹



Size

“small”

$d = 1.5 \mu\text{m}$

“medium”

$d = 5 \mu\text{m}$

“large”

$d = 8 \mu\text{m}$

Q

1850

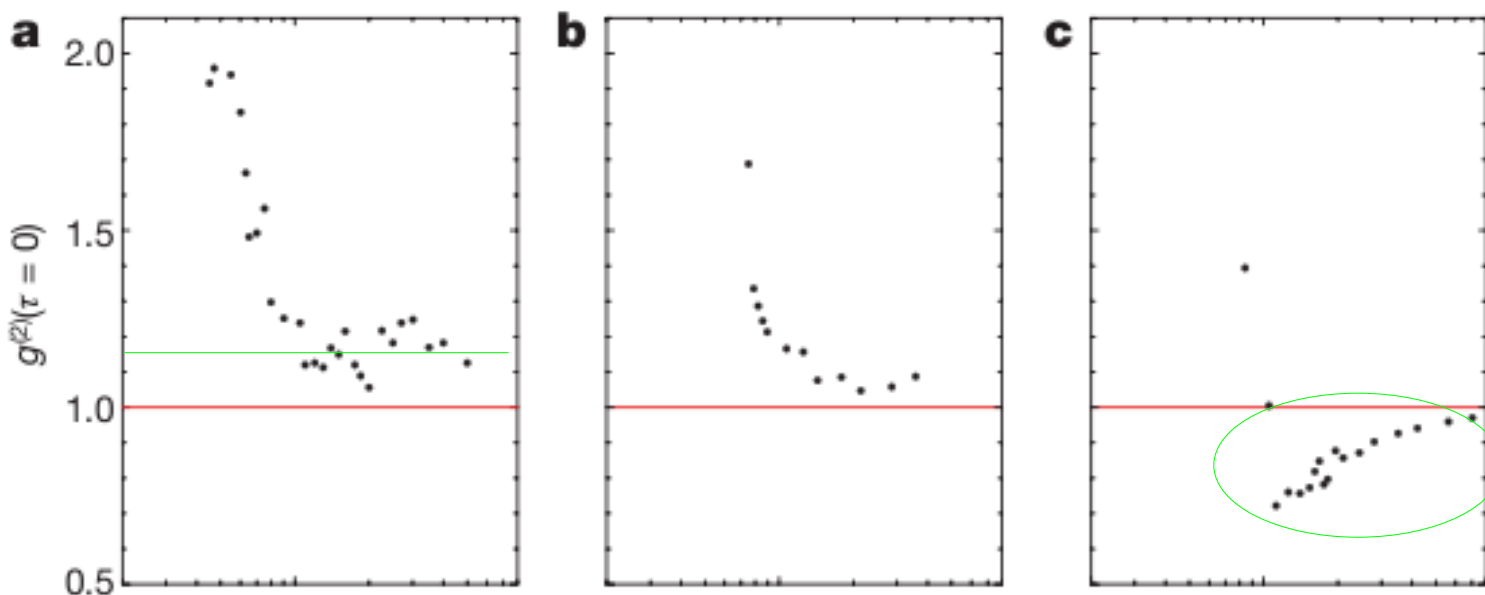
9000

19000

Vol 460 | 9 July 2009 | doi:10.1038/nature08126

Direct observation of correlations between individual photon emission events of a microcavity laser

J. Wiersig^{1†}, C. Gies¹, F. Jahnke¹, M. Aßmann², T. Berstermann², M. Bayer², C. Kistner³, S. Reitzenstein³, C. Schneider³, S. Höfling³, A. Forchel³, C. Kruse¹, J. Kalden¹ & D. Hommel¹



Size

“small”

$d = 1.5 \mu\text{m}$

“medium”

$d = 5 \mu\text{m}$

“large”

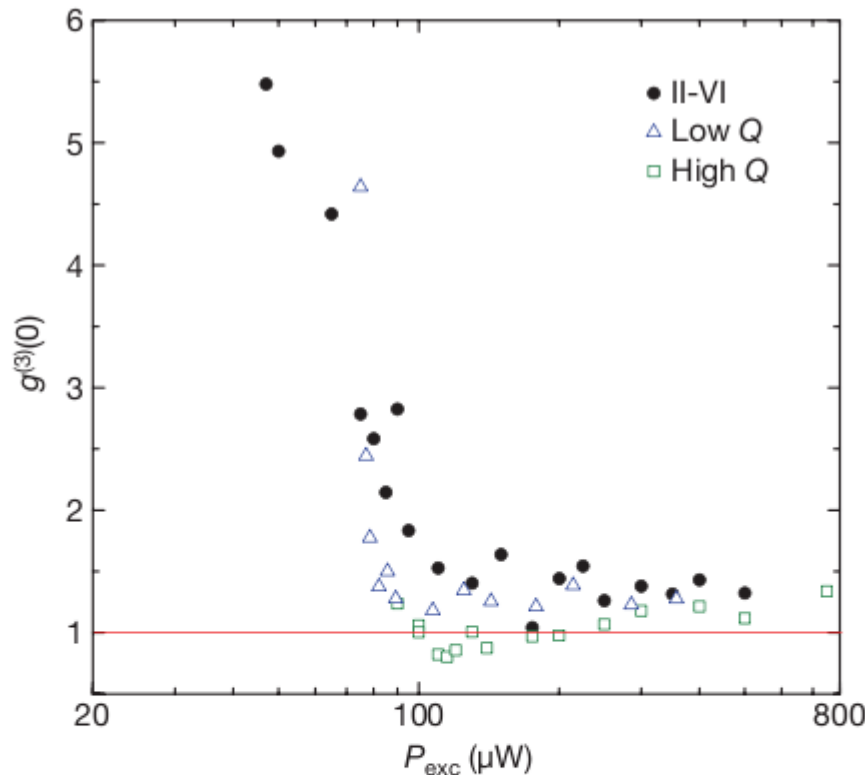
$d = 8 \mu\text{m}$

Q

1850

9000

19000



For the larger laser the $g^{(3)}(0)$ function does not match the theoretically expected values

Coherence?

Figure 5 | Measured third-order correlation function $g^{(3)}(0)$.

Characterization of the simultaneous arrival of three photons as a function of excitation power, for the three different micropillar samples studied in this paper. For the II-VI and low-Q resonators, the time resolution was increased to about 20 ps. These two samples show values close to the theoretical prediction, $g^{(3)}(0) = 6$, at lowest excitation powers. The k th-order correlation functions for a thermal source of radiation are readily obtained from the factorial moments of the Planck distribution, $\langle n(n-1)\cdots(n-k+1) \rangle = k! \langle n \rangle^k$, to give $g^{(k)}(0) = k!$, corresponding to the number of permutations of indistinguishable photons.

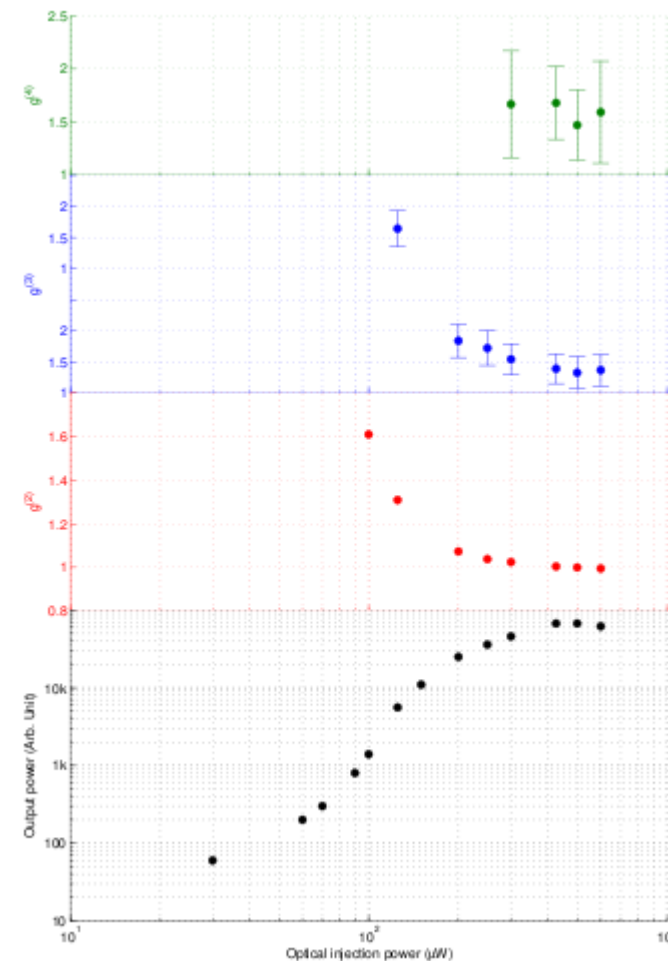
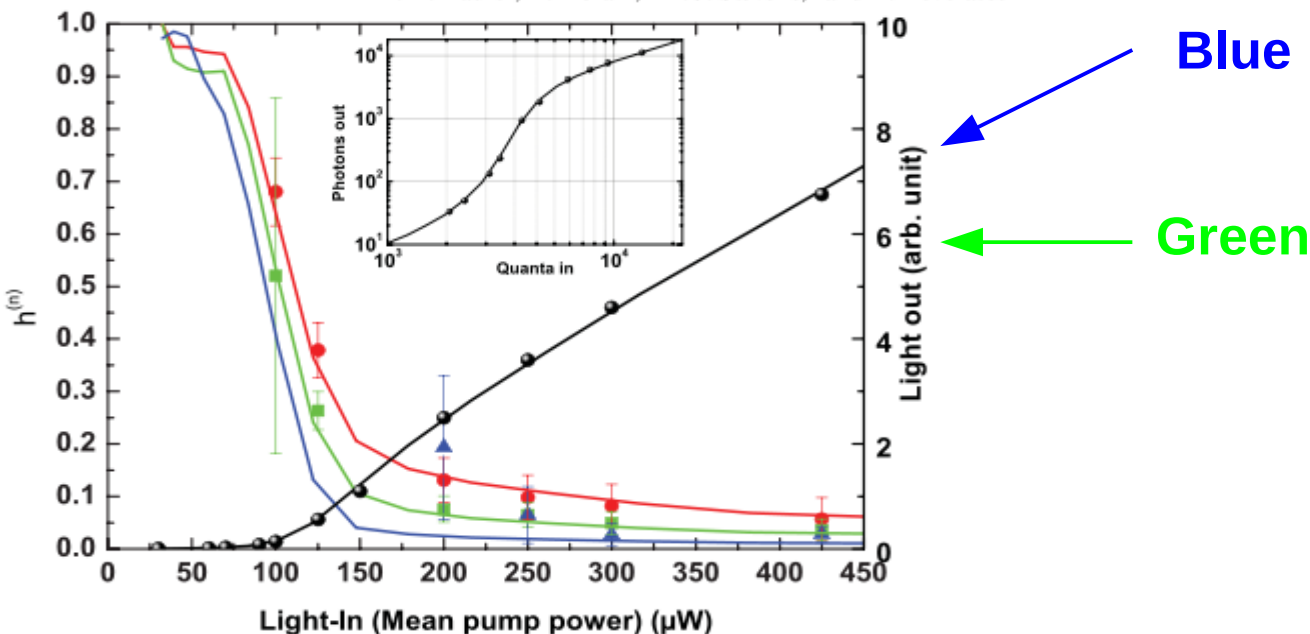
Wiersig et al., Nature **460**, 245 (2009)

RAPID COMMUNICATIONS

PHYSICAL REVIEW A **84**, 061802(R) (2011)

Higher-order photon correlations in pulsed photonic crystal nanolasers

D. Elvira,¹ X. Hachair,¹ V. B. Verma,² R. Braive,¹ G. Beaudoin,¹ I. Robert-Philip,¹ I. Sagnes,¹ B. Bæk,² S. W. Nan
E. A. Dauler,³ I. Abram,¹ M. J. Stevens,² and A. Beveratos^{1,3}



Courtesy of X. Hachair

FIG. 3. (Color online) Right-hand axis: Experimental (black dots) and calculated (black line) light-in–light-out curve. Left-hand axis: Experimental (red circles, green squares, and blue triangles for $n = 2, 3, 4$, respectively) and calculated (continuous lines of the corresponding colors) values of $h^{(n)}$ as functions of pump power. The fit of the $h^{(n)}$ data has no free parameters. Inset: Theoretical light-in–light-out curve in log-log scale. The experimental points have been normalized by the fit parameters.

Photon Statistics of Semiconductor Microcavity Lasers

S. M. Ulrich,^{1,*} C. Gies,² S. Ates,¹ J. Wiersig,² S. Reitzenstein,³ C. Hofmann,³ A. Löffler,³
A. Forchel,³ F. Jahnke,² and P. Michler¹

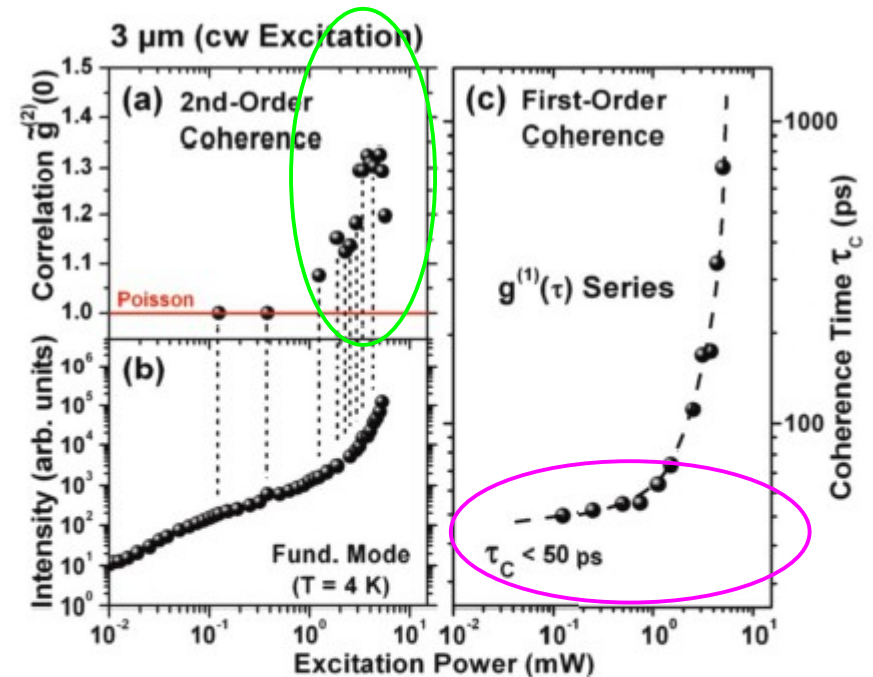
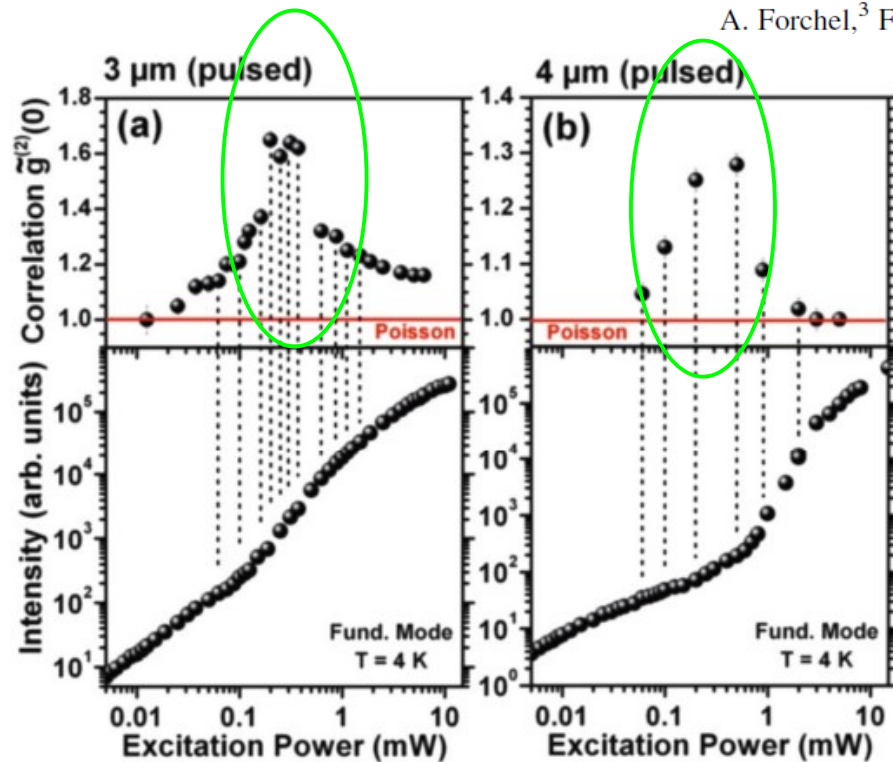


FIG. 4 (color online). (a) $\tilde{g}^{(2)}(\tau = 0)$ autocorrelation results derived from the $3 \mu\text{m}$ pillar fundamental mode under cw excitation [see series in Fig. 2(a)], together with the corresponding mode emission intensity (b). (c) First-order $g^{(1)}(\tau)$ series, revealing a strong τ_c coherence decrease in the low excitation limit.

FIG. 3 (color online). (a),(b) Integrated intensities (bottom) for the 3 ($4 \mu\text{m}$) pillars under nonresonant pulsed excitation. Strong photon bunching $\tilde{g}^{(2)}(0) > 1$ is found from corresponding correlation measurements (top) over a broadened regime around the threshold.

Summary

- $g^{(1)}(t)$ shows very short coherence time
- $g^{(2)}(0)$ remains above 1
drops below 1
shows strong photon bunching ($g^{(2)} > 1$)
- $g^{(3)}(0)$ for larger, high Q, laser inconsistent with theoretical values for thermal light
1.5 μm nanolaser: unsatisfactory convergence
- $g^{(4)}(0)$ “constant” value (1.5 - 2)

III. Statistical mixture

of thermal and coherent light

Does it hold for nano- and microlasers?

Ultrafast tracking of second-order photon correlations in the emission of quantum-dot microresonator lasers

Marc Aßmann, Franziska Veit, and Manfred Bayer

Christopher Gies and Frank Jahnke

Stephan Reitzenstein, Sven Höfling, Lukas Worschech, and Alfred Forchel

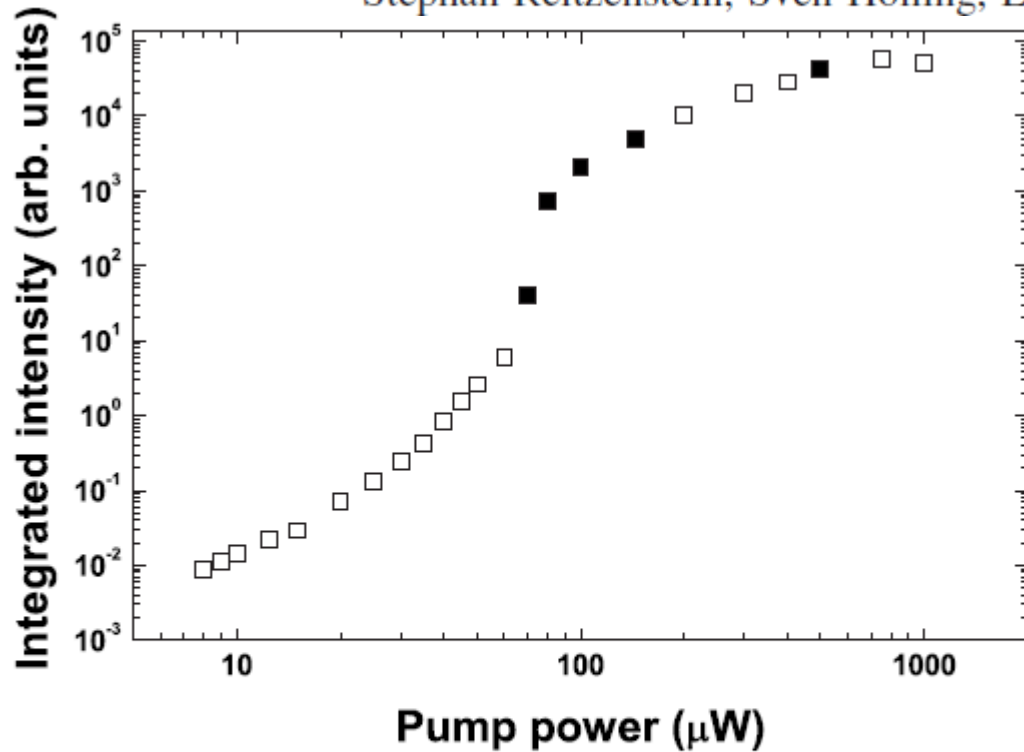
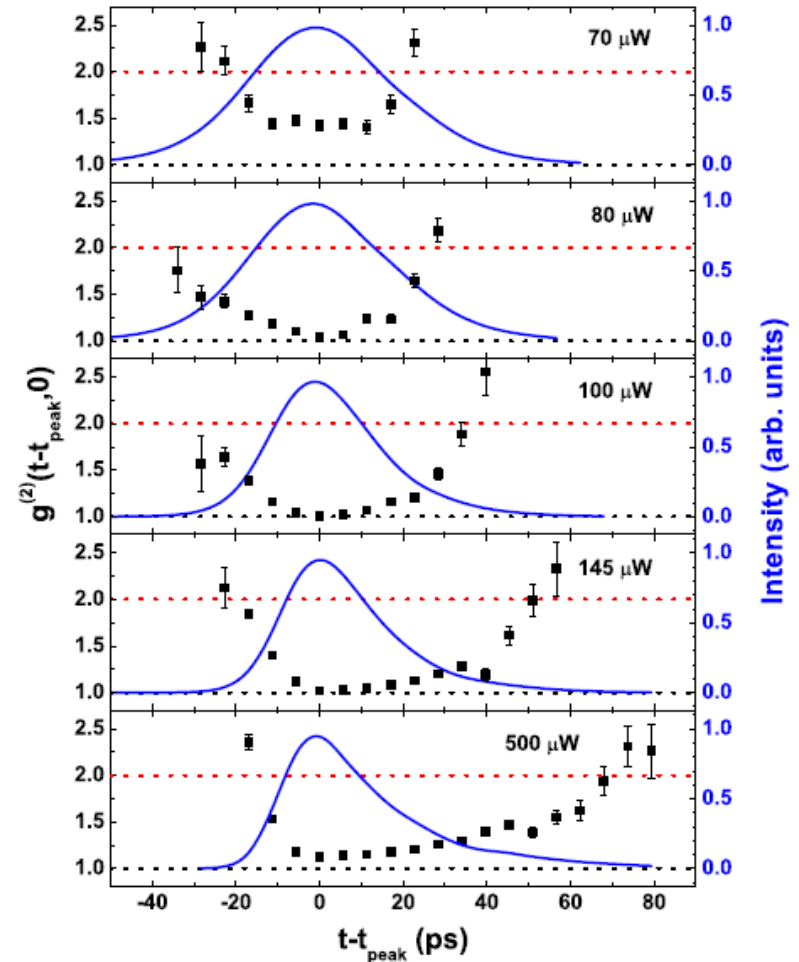


FIG. 1. Integrated intensity of the 6 μm pillar's fundamental mode under nonresonant pulsed excitation. Above threshold, saturation effects become apparent. Filled squares mark the data sets shown in Fig. 2.



Ultrafast tracking of second-order photon correlations in the emission of quantum-dot microresonator lasers

Marc Aßmann, Franziska Veit, and Manfred Bayer

Christopher Gies and Frank Jahnke

Stephan Reitzenstein, Sven Höfling, Lukas Worschech, and Alfred Forchel

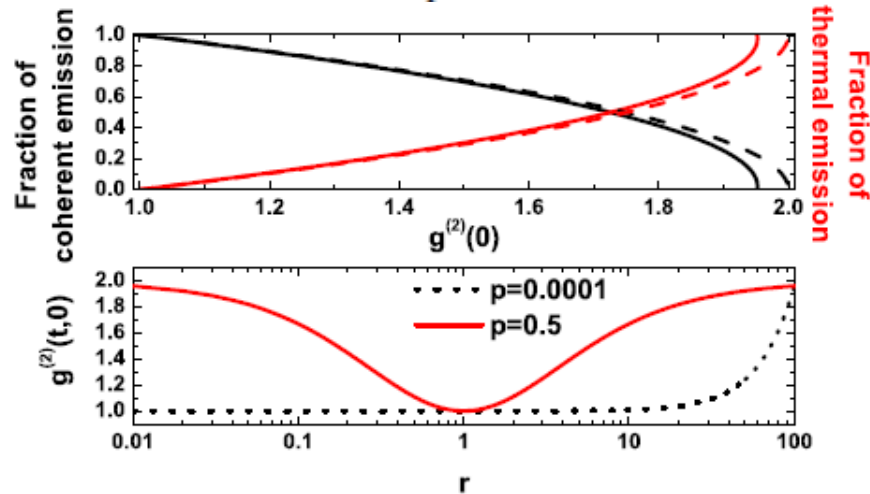
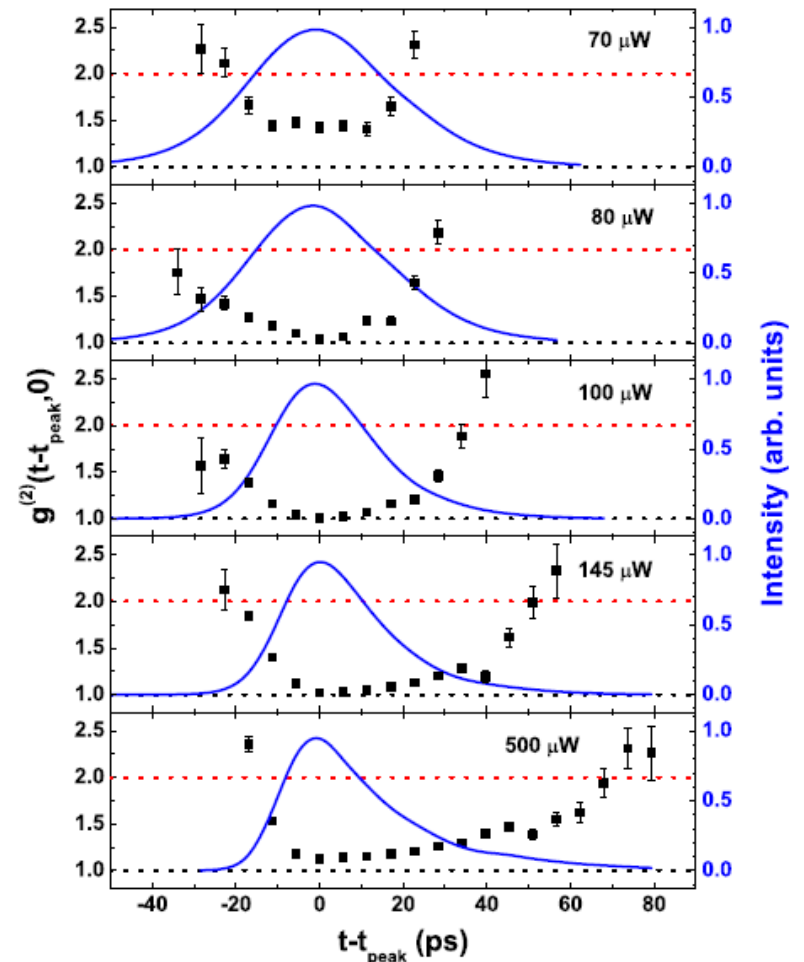


FIG. 3. (Color online) Upper panel: relative fractions of coherent and thermal emission at a fixed $g^{(2)}(t,0)$ as given by a two-mode model (solid lines) compared to the ideal case for infinitely small sampling time (dashed lines). Small deviations occur at high thermal fractions. Lower panel: effect of jitter on the measured $g^{(2)}(t,0)$ for a coherent light pulse depending on the ratio r of the mean photon count rates at the pulse positions connected by the jitter and the relative frequency p of jitter occurrence. While frequent jitter (solid red line) has the same effects for pulse positions with high and low intensity, rare events (dotted black line) only affect regions with low mean photon count rate (high r).



Ultrafast tracking of second-order photon correlations in the emission of quantum-dot microresonator lasers

Marc Aßmann, Franziska Veit, and Manfred Bayer

Christopher Gies and Frank Jahnke

Stephan Reitzenstein, Sven Höfling, Lukas Worschech, and Alfred Forchel

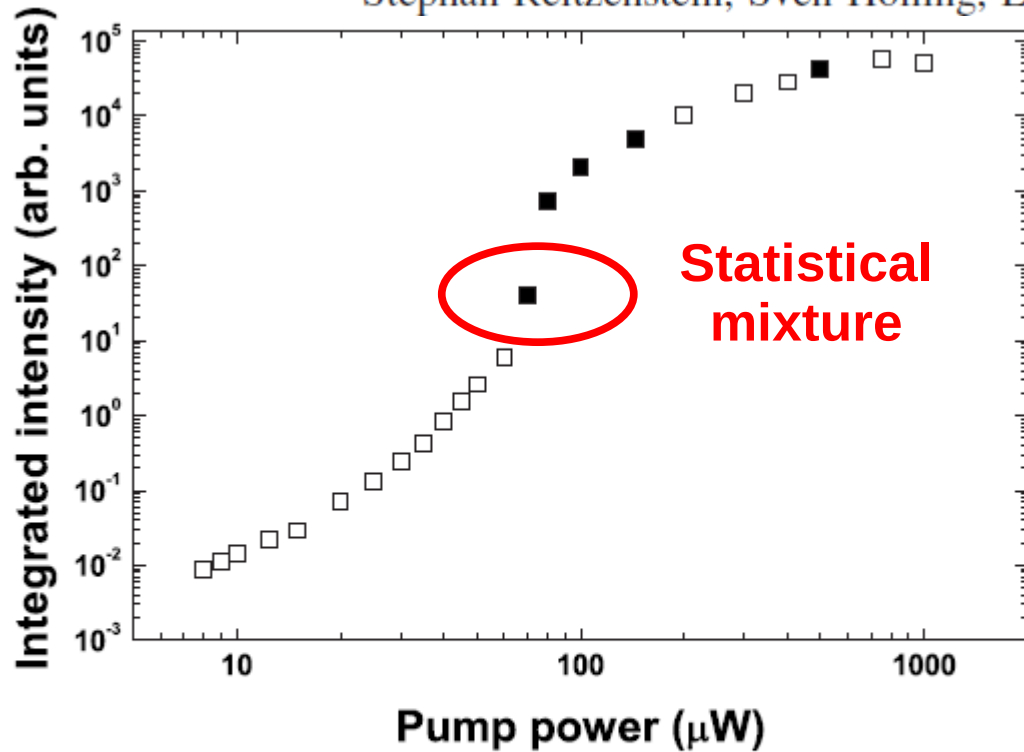
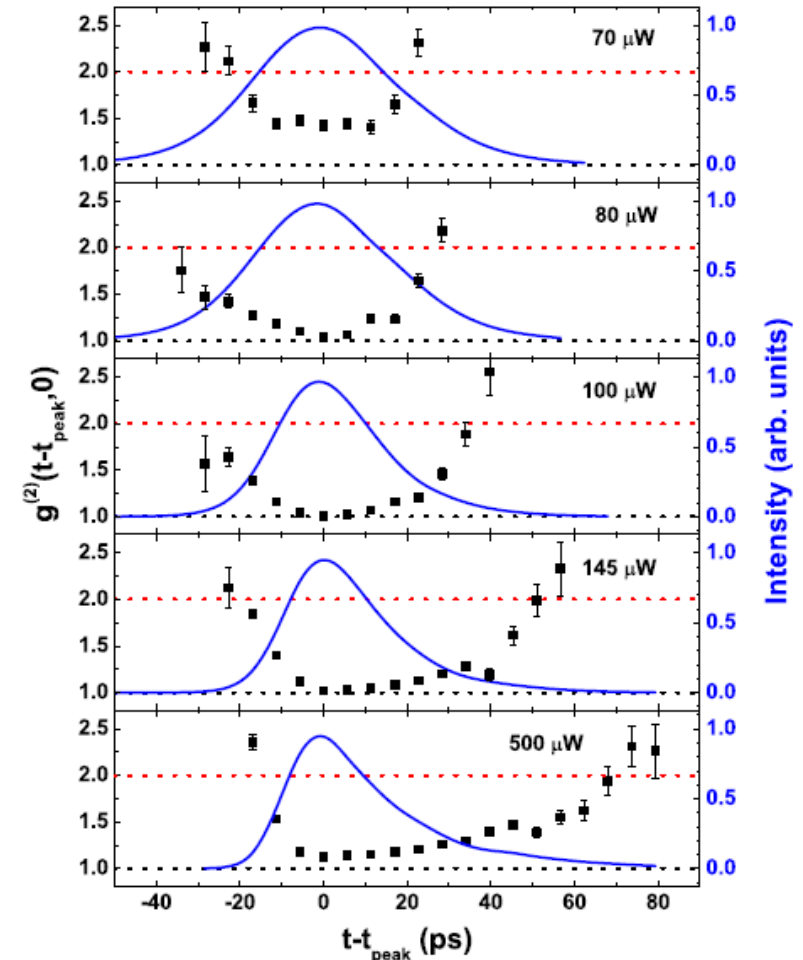


FIG. 1. Integrated intensity of the 6 μm pillar's fundamental mode under nonresonant pulsed excitation. Above threshold, saturation effects become apparent. Filled squares mark the data sets shown in Fig. 2.



PHYSICAL REVIEW A **88**, 013801 (2013)

Theory of interferometric photon-correlation measurements: Differentiating coherent from chaotic light

A. Lebreton, I. Abram, R. Braive, I. Sagnes, I. Robert-Philip,* and A. Beveratos

Measure average correlation in a scanning Michelson interferometer

$$\hat{E}_A^*(t) = E_0^* \frac{a^\dagger(t + d/c) - a^\dagger(t)}{\sqrt{2}}, \quad + \text{h.c.} \quad (4)$$

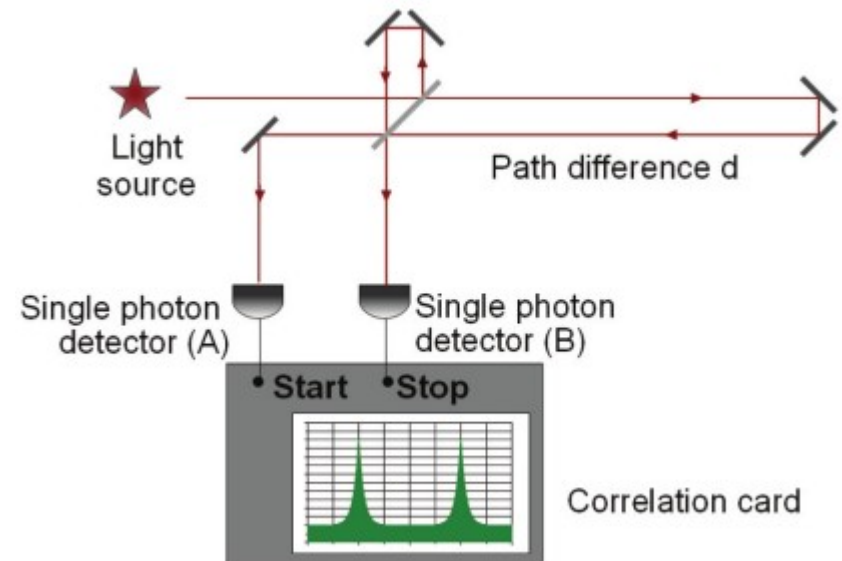
$$\hat{E}_B^*(t) = E_0^* \frac{a^\dagger(t + d/c) + a^\dagger(t)}{\sqrt{2}},$$

$$\langle \hat{E}_A^*(t) E_A(t) \rangle = \frac{I_1}{2} \{1 - 2 \text{Re}[g^{(1)}(d/c)]\}, \quad (5)$$

$$\langle \hat{E}_B^*(t) E_B(t) \rangle = \frac{I_1}{2} \{1 + 2 \text{Re}[g^{(1)}(d/c)]\},$$

Compute normalized correlation:

$$g^{(2X)}(\tau, d/c) = \langle \hat{E}_A^*(0) \hat{E}_B^*(\tau) \hat{E}_B(\tau) \hat{E}_A(0) \rangle, \quad (6)$$



Technique borrowed from
Photon-correlation Fourier Spectroscopy
X. Brockmann *et al.*, Opt. Expr. **14**, 6333 (2006)

PHYSICAL REVIEW A **88**, 013801 (2013)

Theory of interferometric photon-correlation measurements: Differentiating coherent from chaotic light

A. Lebreton, I. Abram, R. Braive, I. Sagnes, I. Robert-Philip,* and A. Beveratos

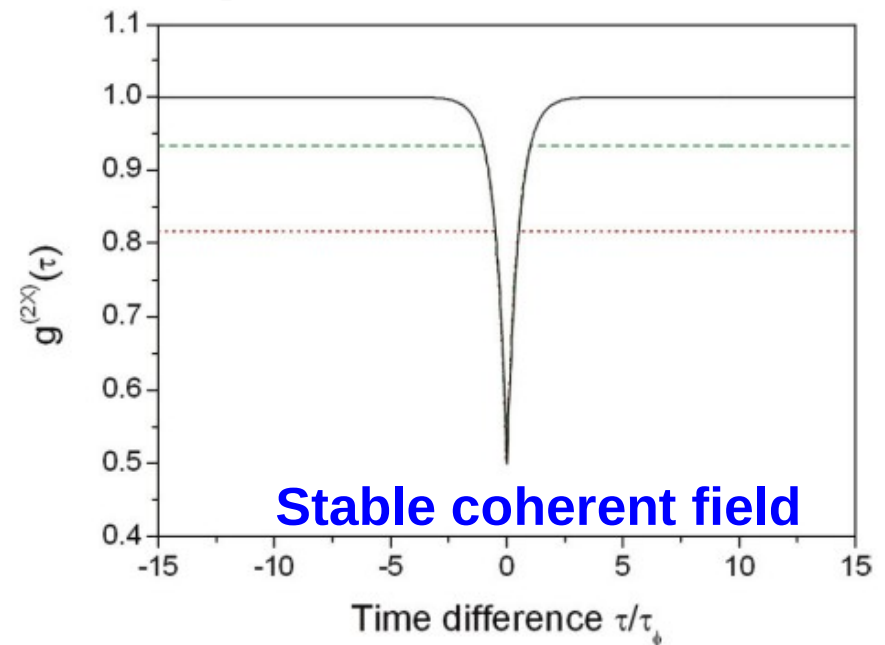
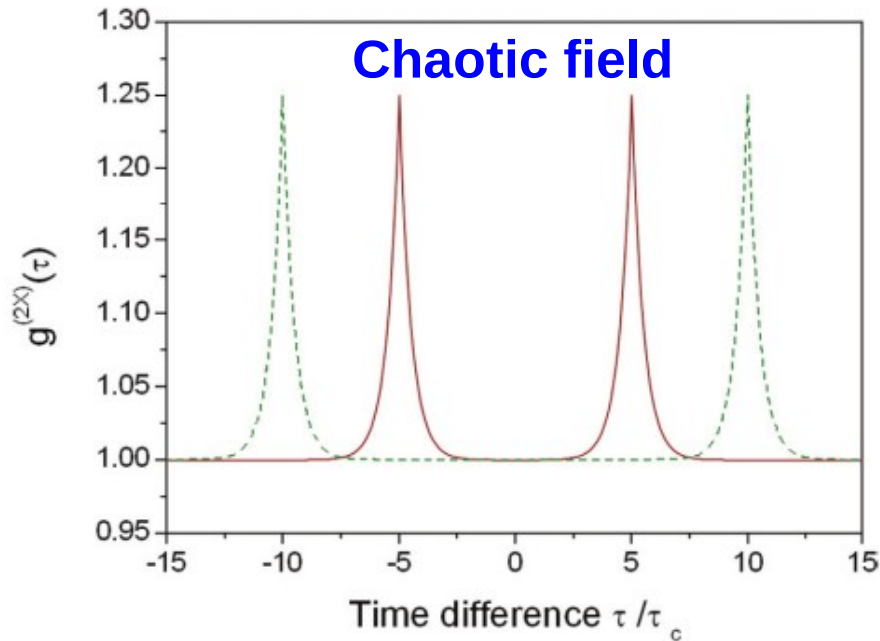


FIG. 2. (Color online) Interferometric second-order intensity cross-correlation function for a chaotic field $g_{\text{chaotic}}^{(2X)}(\tau, d/c)$ at the output ports of an unbalanced Michelson (or Mach-Zehnder) interferometer with pathlength difference $d = 5c\tau_c$ (continuous red curve) and $d = 10c\tau_c$ (dashed green curve).

FIG. 3. (Color online) Interferometric second-order intensity cross-correlation function for a stable coherent wave $g_{\text{coh}}^{(2X)}(\tau, d/c)$ at the output ports of an unbalanced Michelson (or Mach-Zehnder) interferometer with pathlength difference $d = 0.5c\tau_\phi$ (dotted red curve), $d = c\tau_\phi$ (dashed green curve), and $d \gg c\tau_c$ (continuous black curve).

Theory of interferometric photon-correlation measurements: Differentiating coherent from chaotic light

A. Lebreton, I. Abram, R. Braive, I. Sagnes, I. Robert-Philip,* and A. Beveratos

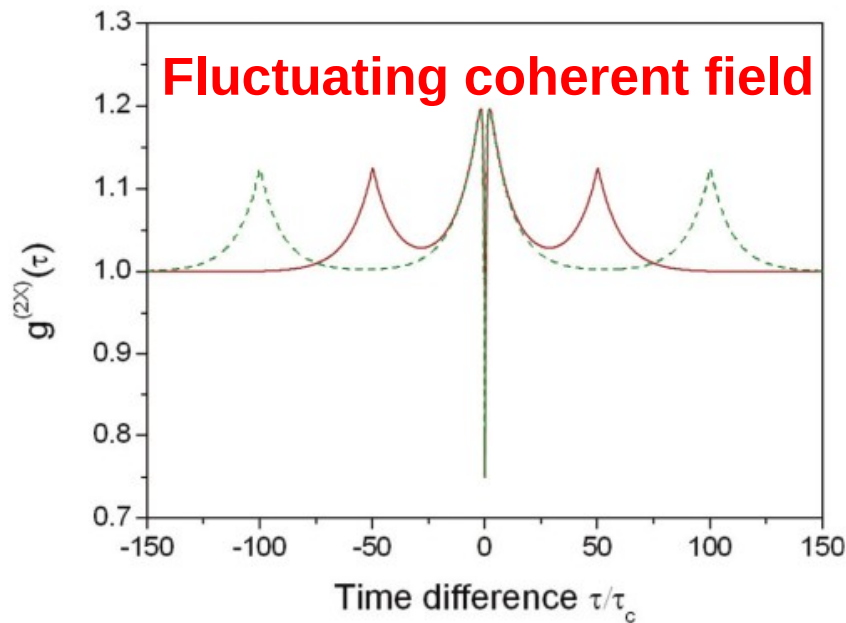


FIG. 4. (Color online) Interferometric second-order intensity cross-correlation function for a coherent field with intensity fluctuations $g_{\text{amp-fluct}}^{(2X)}(\tau, d/c)$ at the output ports of an unbalanced Michelson (or Mach-Zehnder) interferometer with pathlength difference $d = 50c\tau_c = 5c\tau_{\text{int}}$ (continuous red curve), $d = 100c\tau_c = 10c\tau_{\text{int}}$ (dashed green curve). The characteristic time of the intensity fluctuations is taken to be $\tau_{\text{int}} = 10\tau_c$.

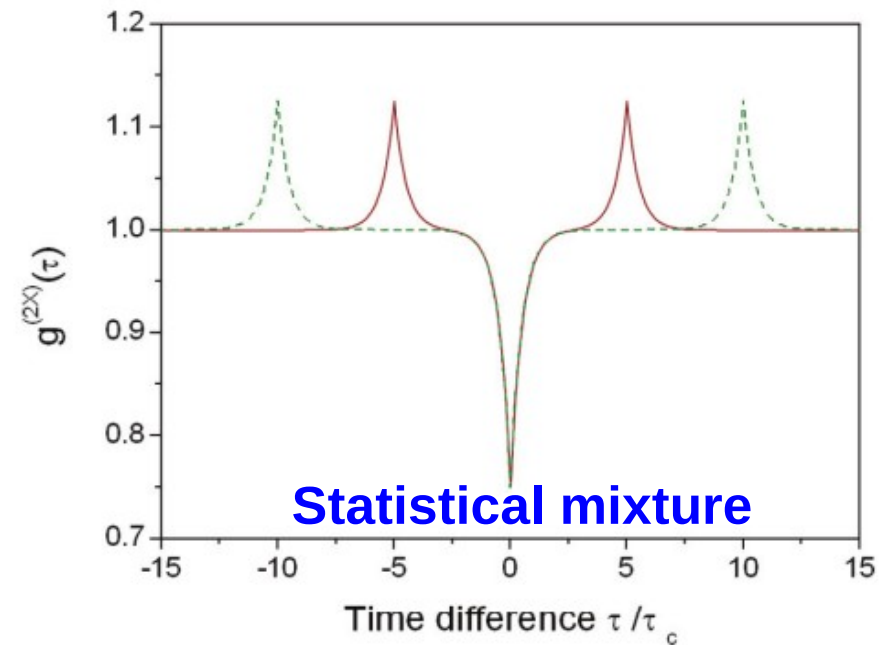


FIG. 5. (Color online) Interferometric second-order intensity cross-correlation function for a 50:50 “mixture” of coherent and chaotic light $g_{\text{mix}}^{(2X)}(\tau, d/c)$ at the output ports of an unbalanced Michelson (or Mach-Zehnder) interferometer with pathlength difference $d = 5c\tau_c$ (continuous red curve), $d = 10c\tau_c$ (dashed green curve), and $\tau_\phi = \tau_c$.

Unequivocal Differentiation of Coherent and Chaotic Light through Interferometric Photon Correlation Measurements

A. Lebreton, I. Abram, R. Braive, I. Sagnes, I. Robert-Philip,* and A. Beveratos

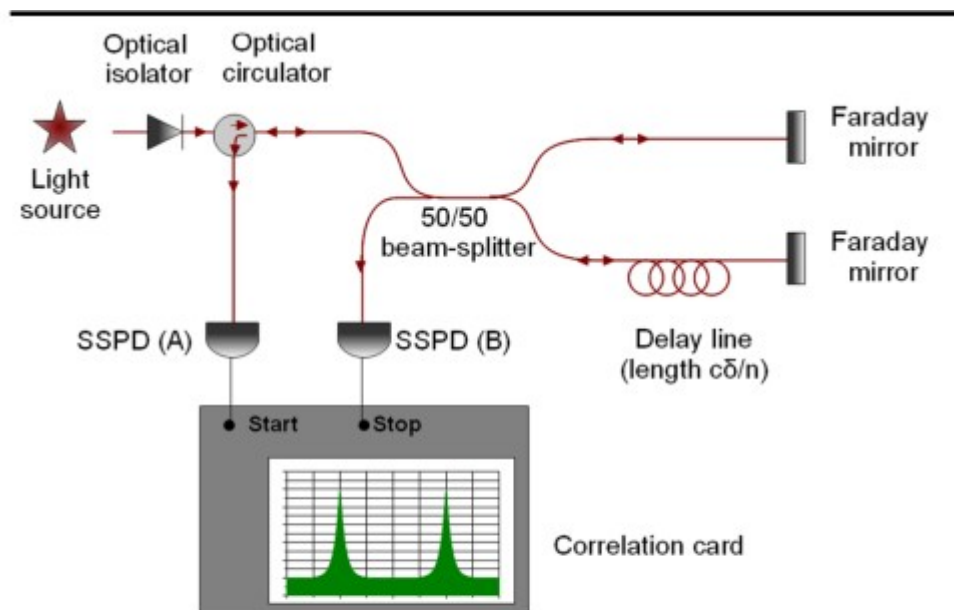


FIG. 1 (color online). Experimental setup. Light is sent into an unbalanced Michelson interferometer made of optical fibers. Two single photon detectors (SSPDs) measure the cross correlations between the two output ports of the interferometer.

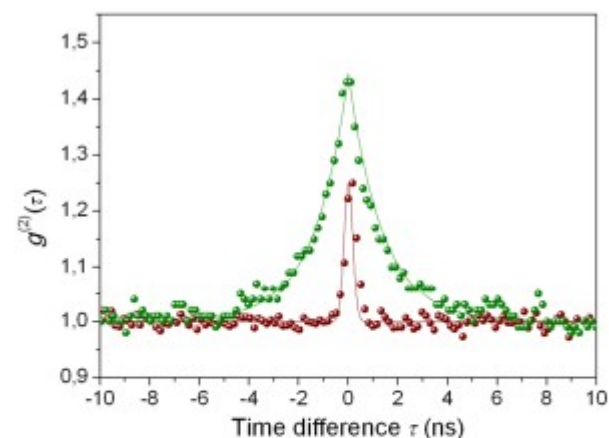
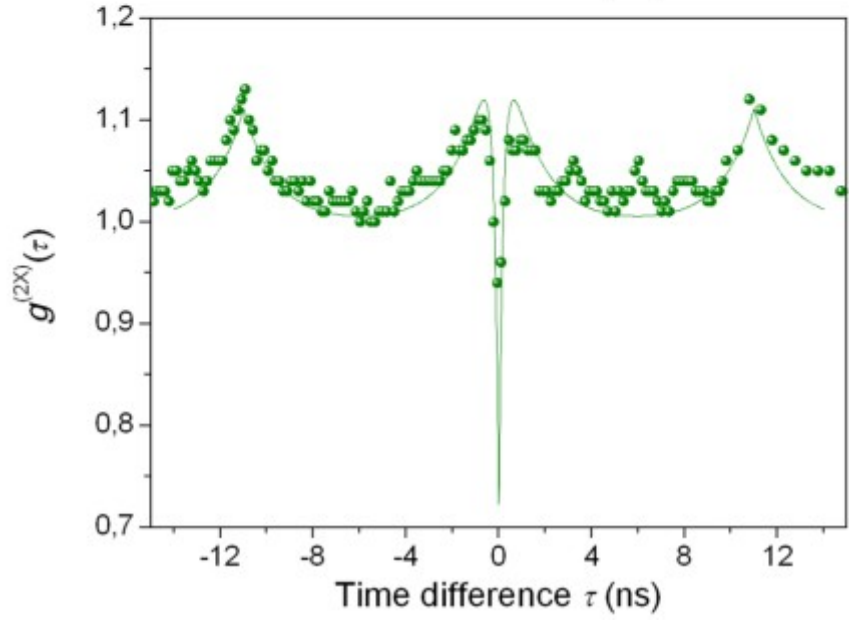
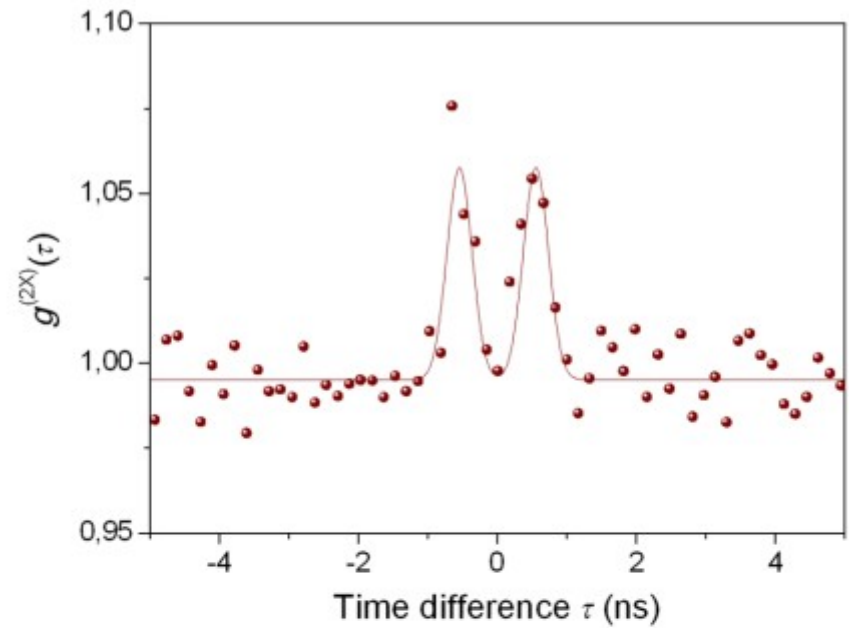


FIG. 2 (color online). Second order autocorrelation function $g^{(2)}(\tau)$ of a nanoscale laser pumped at $1.1 P_{th}$ [green (gray) dots and curve] and a filtered chaotic source [red (black) dots and curve]. The points are experimental data and the continuous curves are fits to Eqs. (6) and (9).

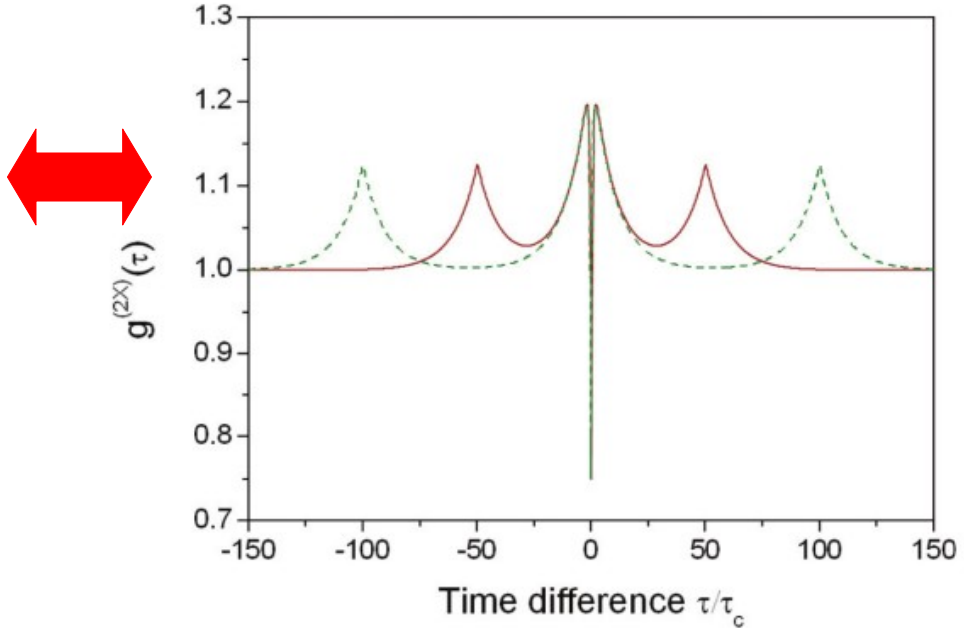
Photon-correlation Fourier spectroscopy



2013) PHYSICAL REVIEW LETTERS week ending 19 APRIL 2013

Unequivocal Differentiation of Coherent and Chaotic Light through Interferometric Photon Correlation Measurements

A. Lebreton, I. Abram, R. Braive, I. Sagnes, I. Robert-Philip,* and A. Beveratos



Summary

Contradicting information coming from two different experiments

1. In the “intermediate threshold region” a statistical superposition of chaotic light (spontaneous emission) and coherent light (laser) is emitted by the device
2. The light emitted by the device is coherent, but exhibits (strong) amplitude fluctuations

Comparison between the two experiments difficult:

Pulsed regime
Entirely different devices
Reproducibility of samples

IV. Oscillations in coherence function

**Experiments and theory in
Microcavities and nanocavities**

Vol 460 | 9 July 2009 | doi:10.1038/nature08126

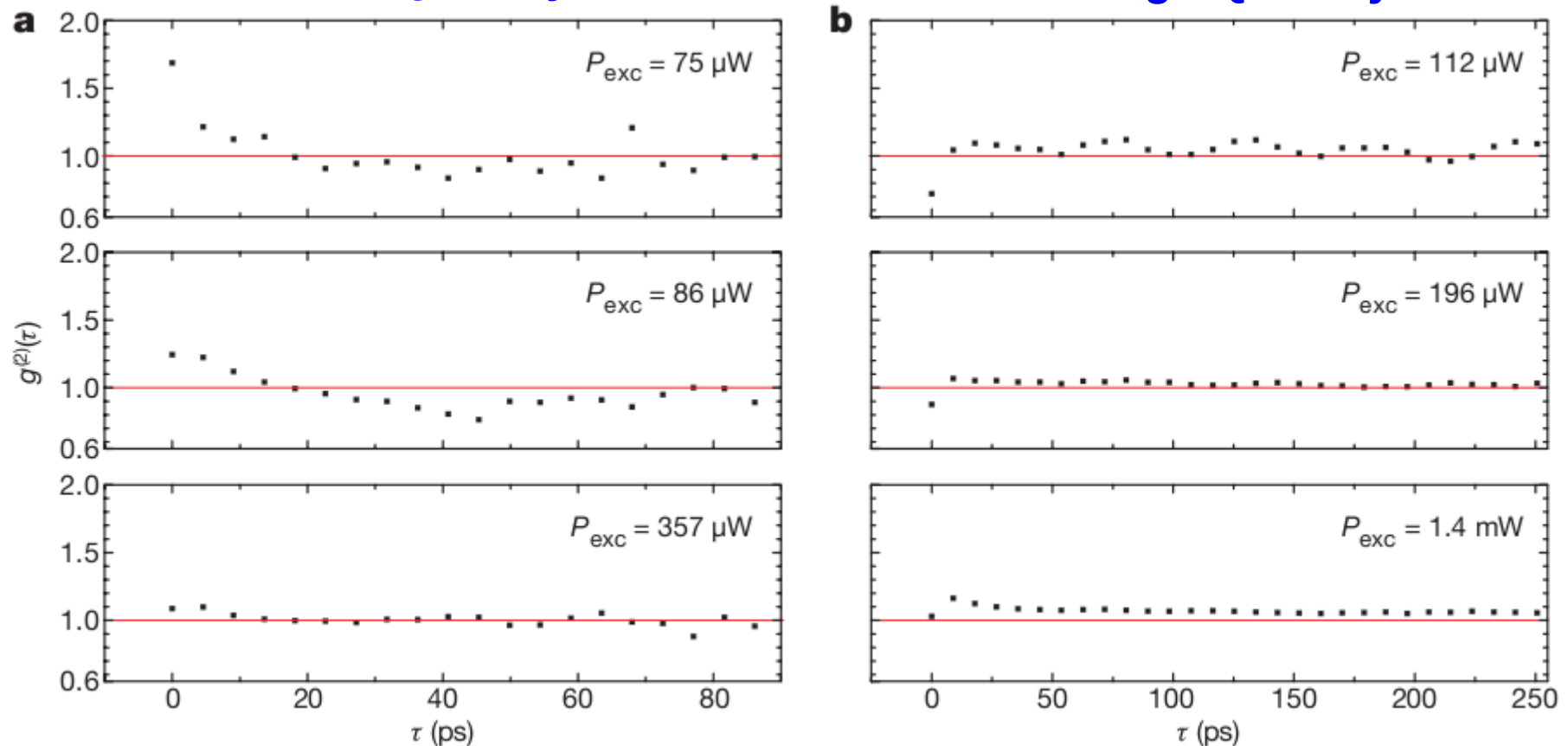
Direct observation of correlations between individual photon emission events of a microcavity laser

Nanolaser

J. Wiersig^{1†}, C. Gies¹, F. Jahnke¹, M. Aßmann², T. Berstermann², M. Bayer², C. Kistner³, S. Reitzenstein³, C. Schneider³, S. Höfling³, A. Forchel³, C. Kruse¹, J. Kalden¹ & D. Hommel¹

Low Q cavity

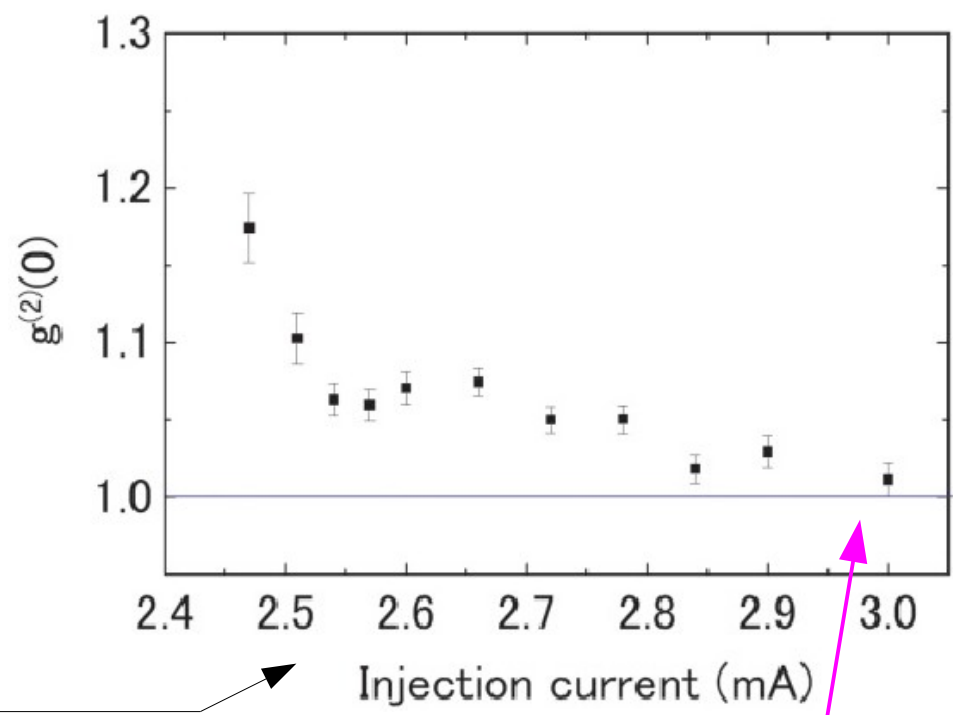
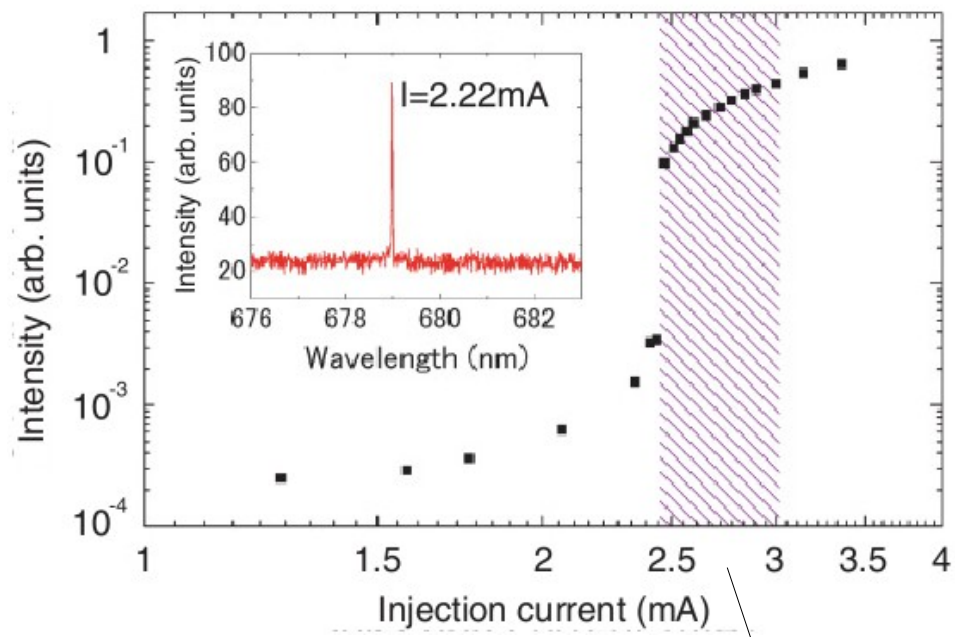
High Q cavity



PHYSICAL REVIEW A **85**, 053811 (2012)

Fast periodic modulations in the photon correlation of single-mode vertical-cavity surface-emitting lasers

Naotomo Takemura,¹ Junko Omachi,² and Makoto Kuwata-Gonokami^{2,3,*} *Microlaser*



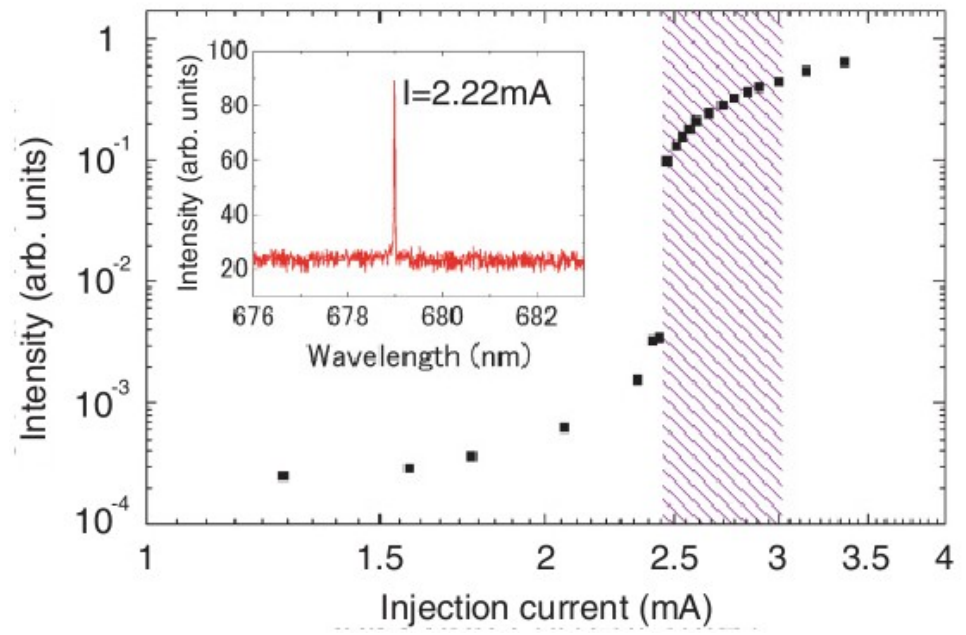
coherence

PHYSICAL REVIEW A 85, 053811 (2012)

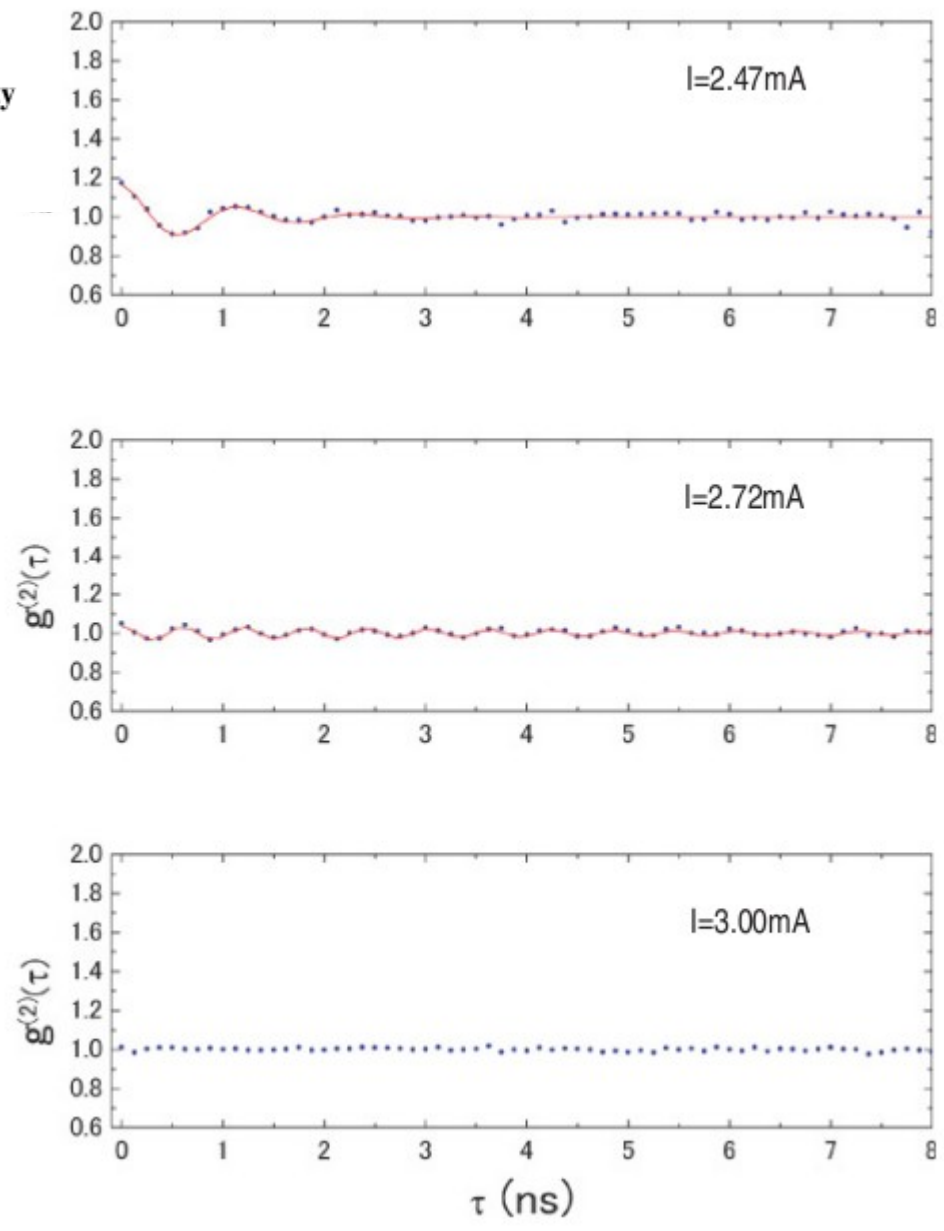
Fast periodic modulations in the photon correlation of single-mode vertical-cavity surface-emitting lasers

Naotomo Takemura,¹ Junko Omachi,² and Makoto Kuwata-Gonokami^{2,3,*}

Microlaser



Oscillations in coherence



New Journal of Physics

The open access journal for physics

2013 New J. Phys. 15 033039

Stochastically sustained population oscillations in high- β nanolasers

A Lebreton¹, I Abram¹, N Takemura², M Kuwata-Gonokami^{2,3},
I Robert-Philip^{1,4} and A Beveratos¹

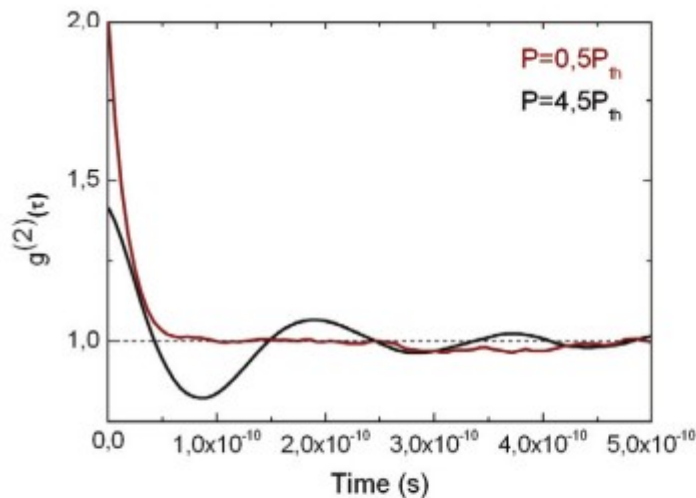


Figure 3. Second-order photon correlation function $g^{(2)}(\tau)$ of a nanolaser ($\beta = 0.25$) undergoing photon population cycles, for $P = 0.5 P_{th}$ (red line) and $P = 4.5 P_{th}$ (black line). The dashed horizontal line corresponds to $g^{(2)}(\tau) = 1$, the value in continuous-wave lasers.

$$g^{(2)}(\tau) = 1 + |g^{(1)}(\tau)|^2$$

**Violation of Siegert relation
(through population oscillations)**

**Numerical: Rate Equations
(discrete variables)**

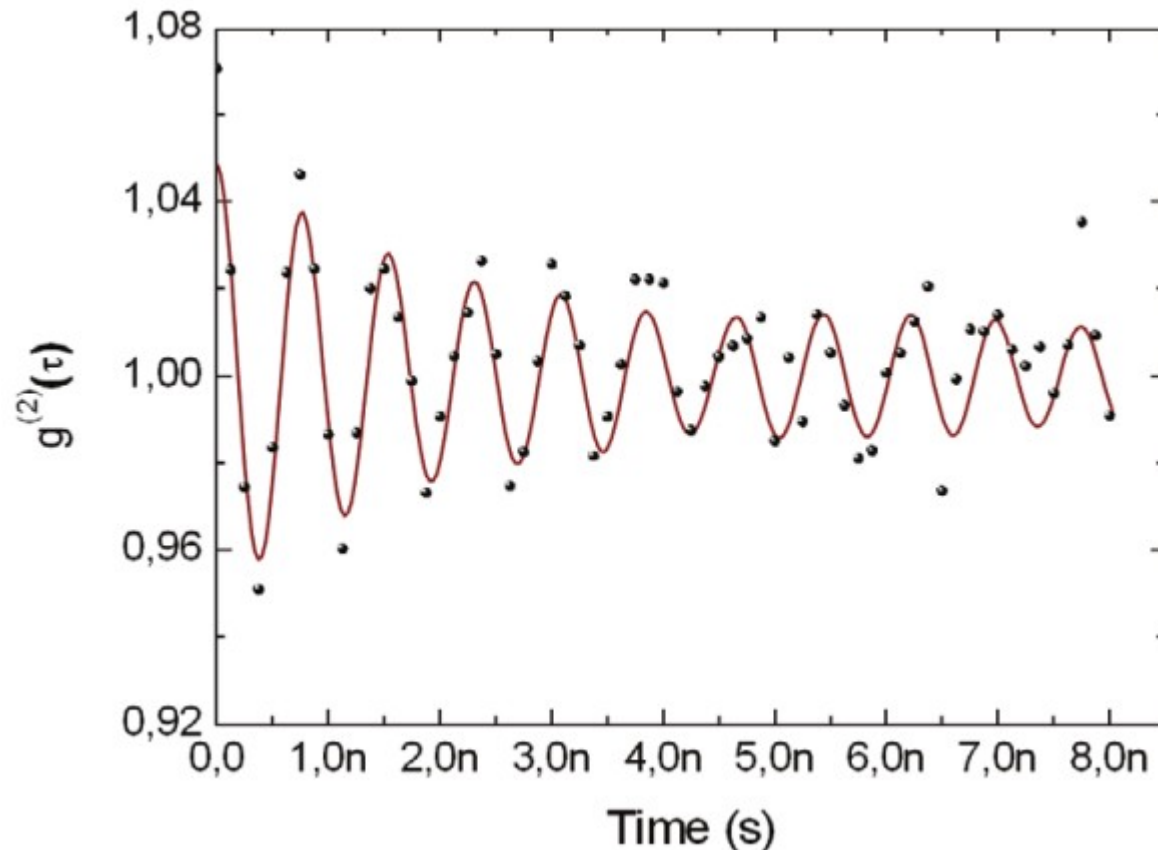
New Journal of Physics

The open access journal for physics

2013 New J. Phys. 15 033039

Stochastically sustained population oscillations in high- β nanolasers

A Lebreton¹, I Abram¹, N Takemura², M Kuwata-Gonokami^{2,3},



Experimental data from
Phys. Rev. A 85, 053811 (2012)

Rate equations simulations
(discrete variables)

Summary

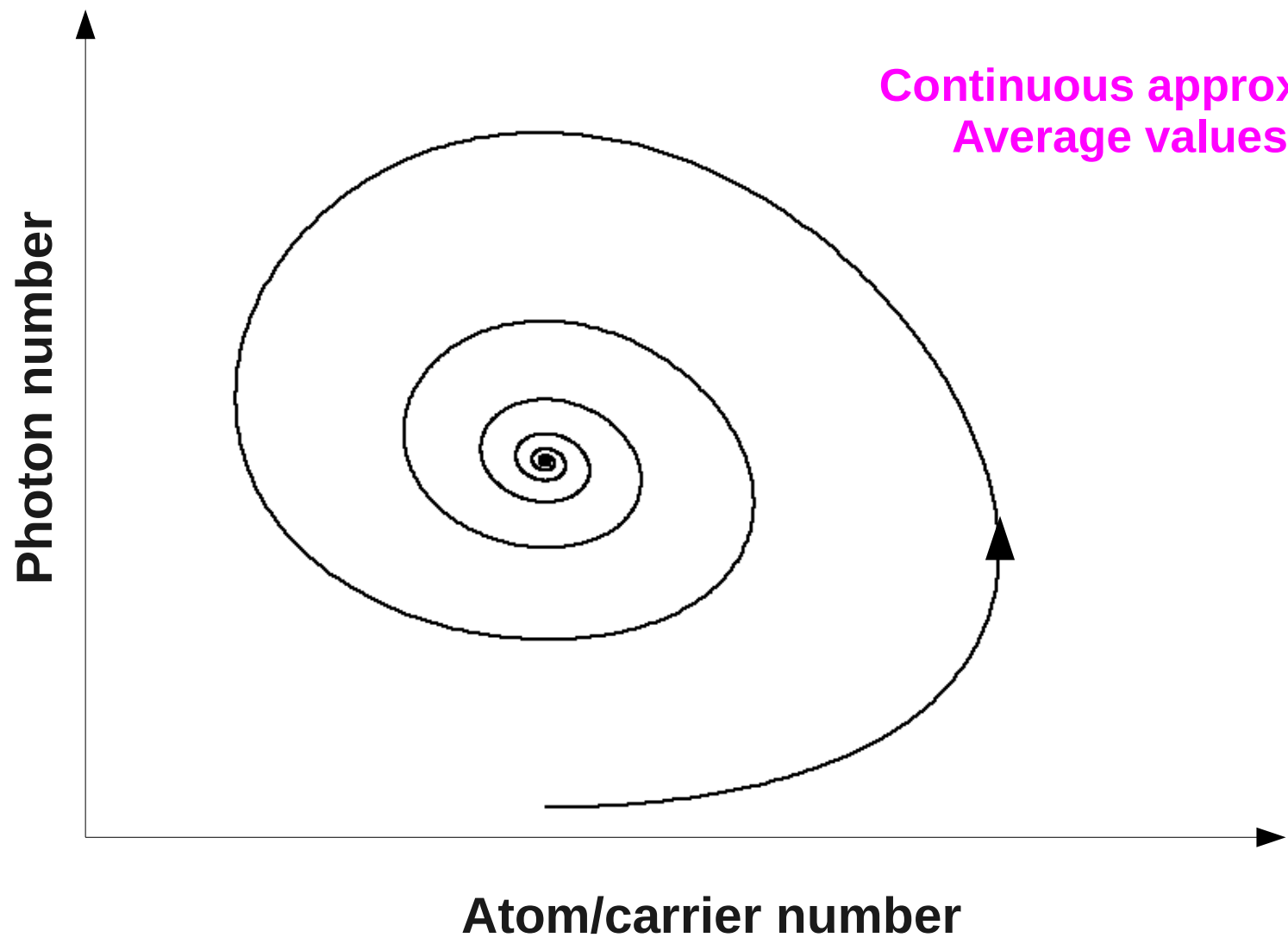
**Oscillations in coherence $g^{(2)}(\tau)$ appear both
in (some) nanolasers
in microlasers**

**Result from coherent oscillations between population and
e.m. field**

**Can give rise to misinterpretation of $g^{(2)}(\tau=0)$ as imperfect
coherence**

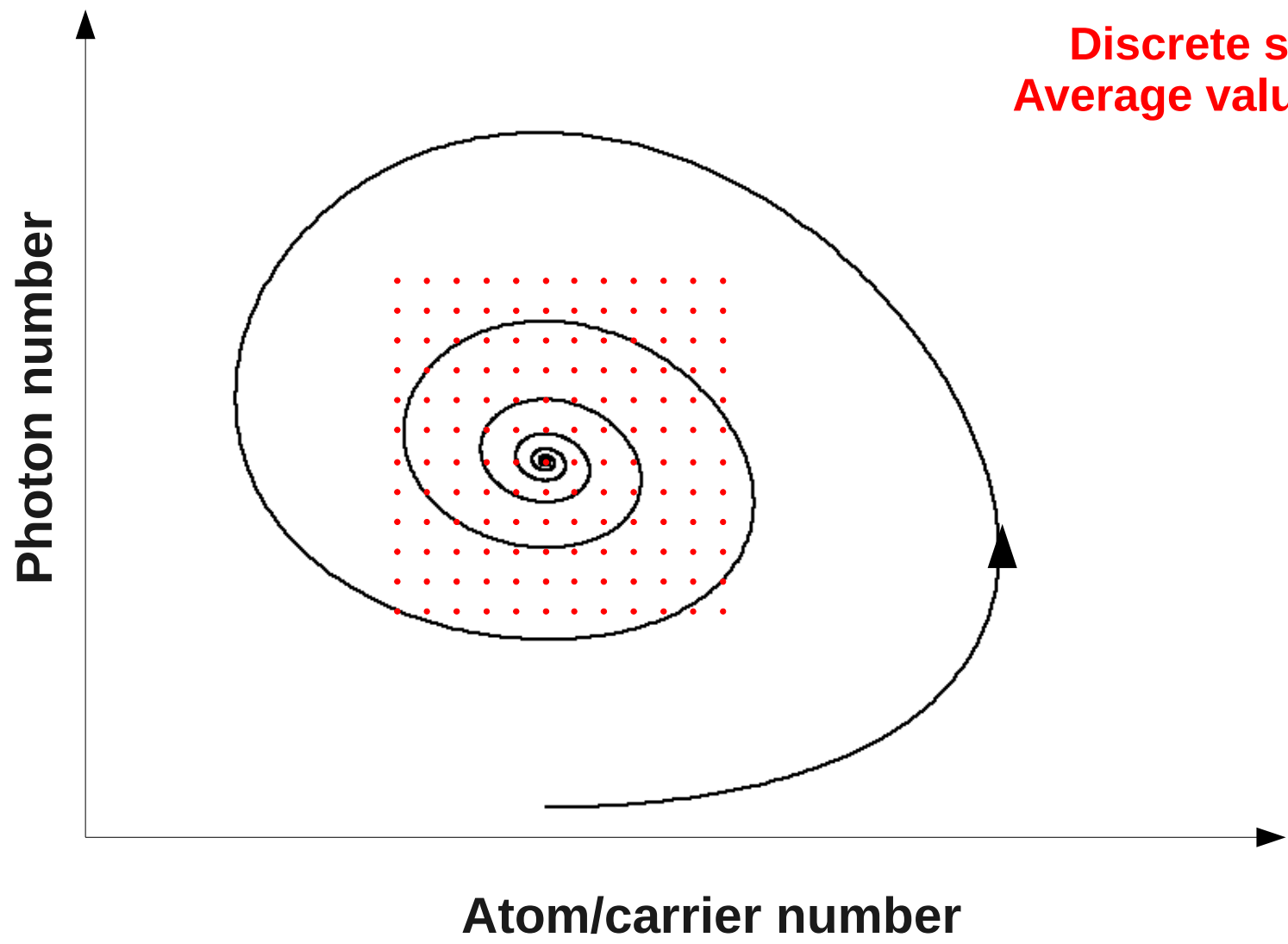
V. Additional remarks

Origin of oscillations



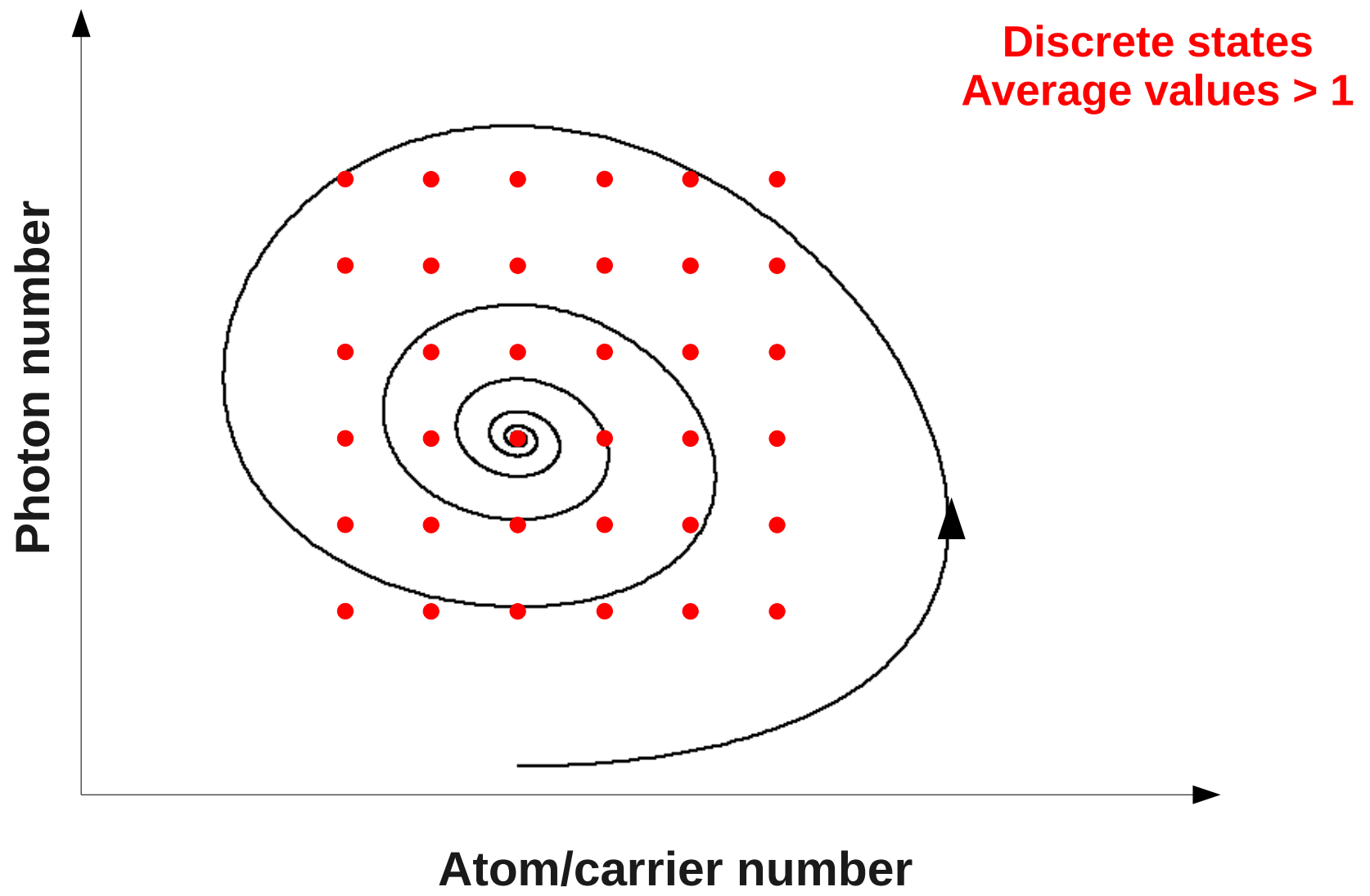
Continuous approximation
Average values $\gg 1$

Origin of oscillations

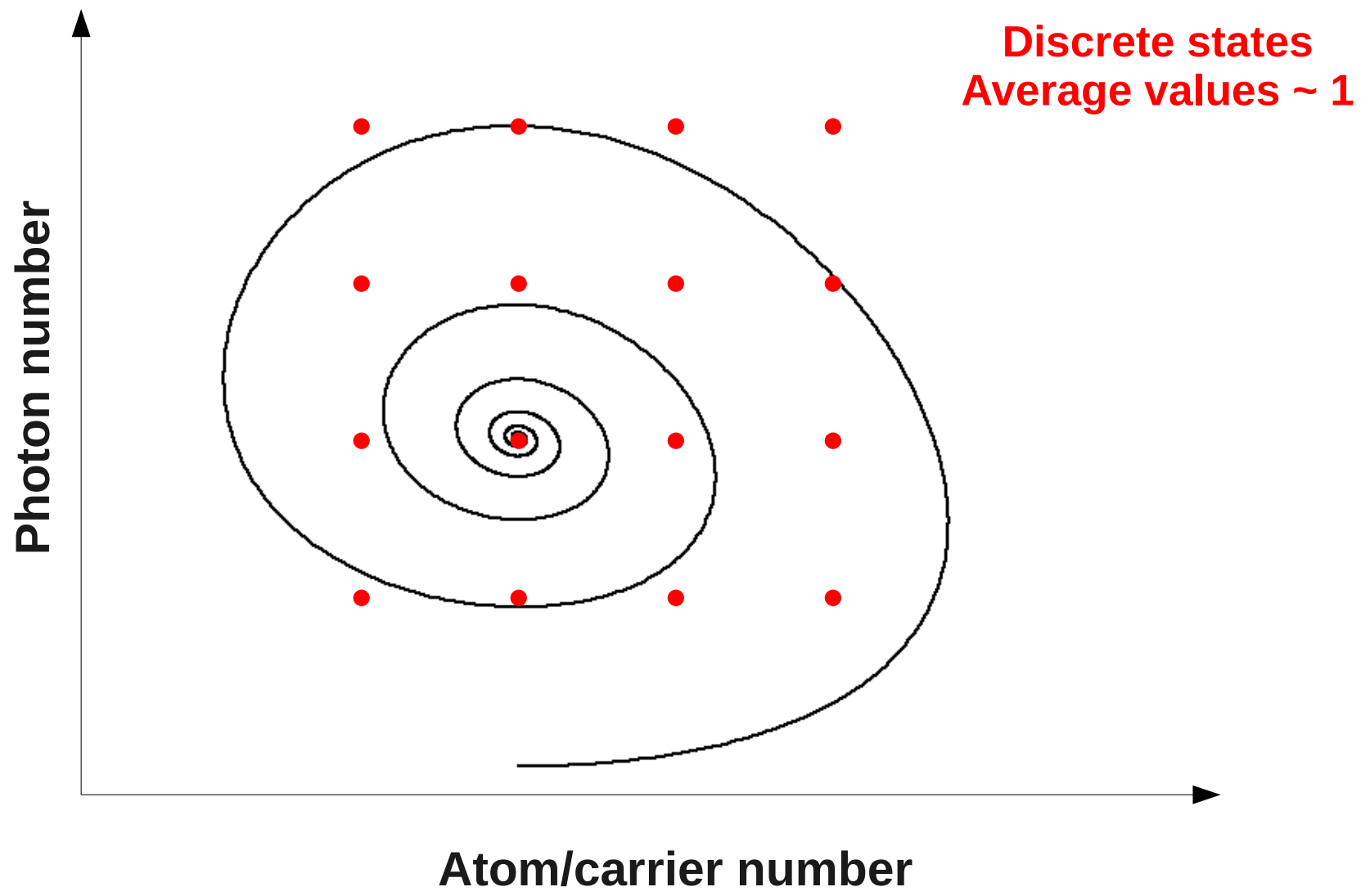


Discrete states
Average values $\gg 1$

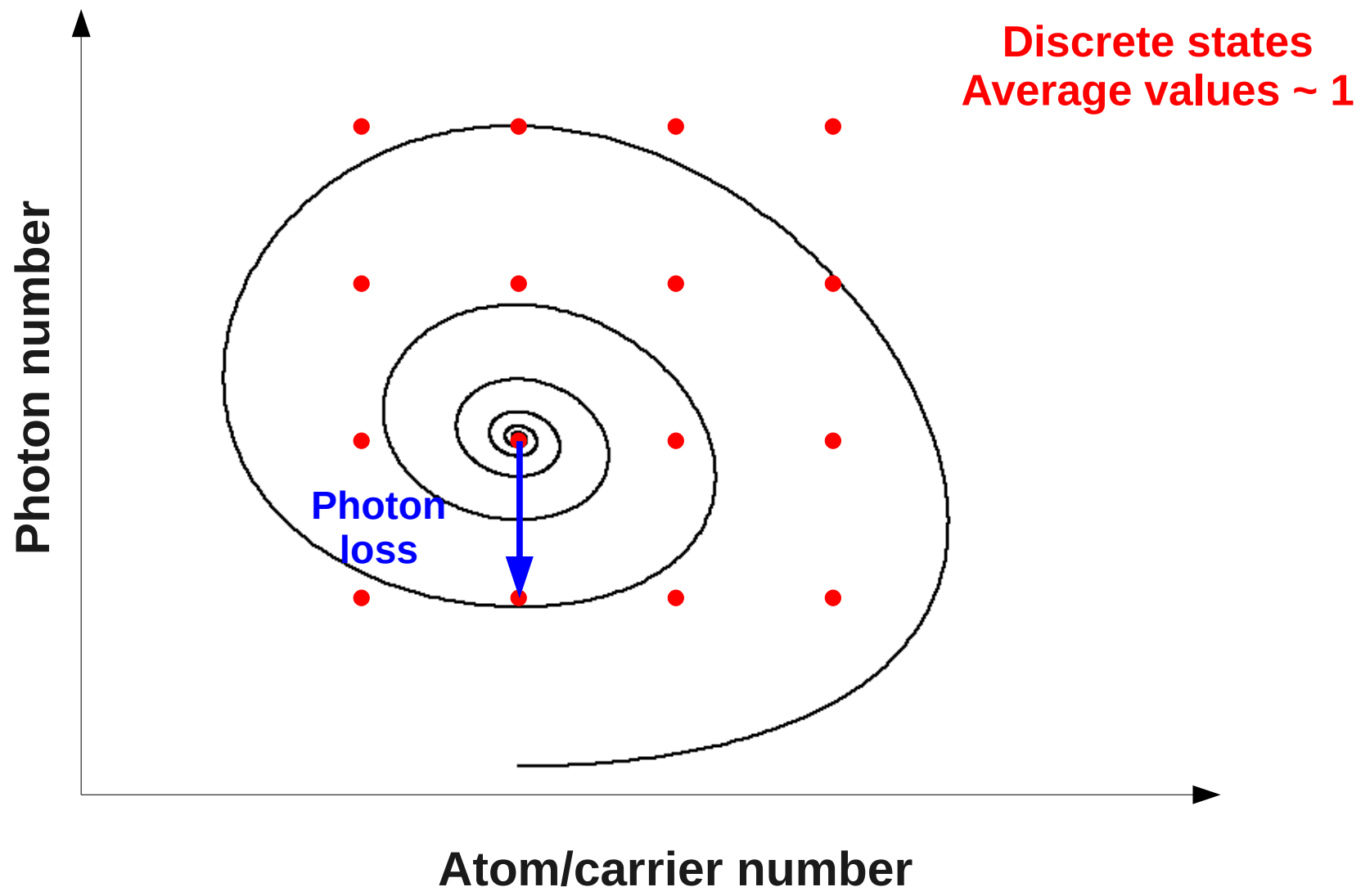
Origin of oscillations



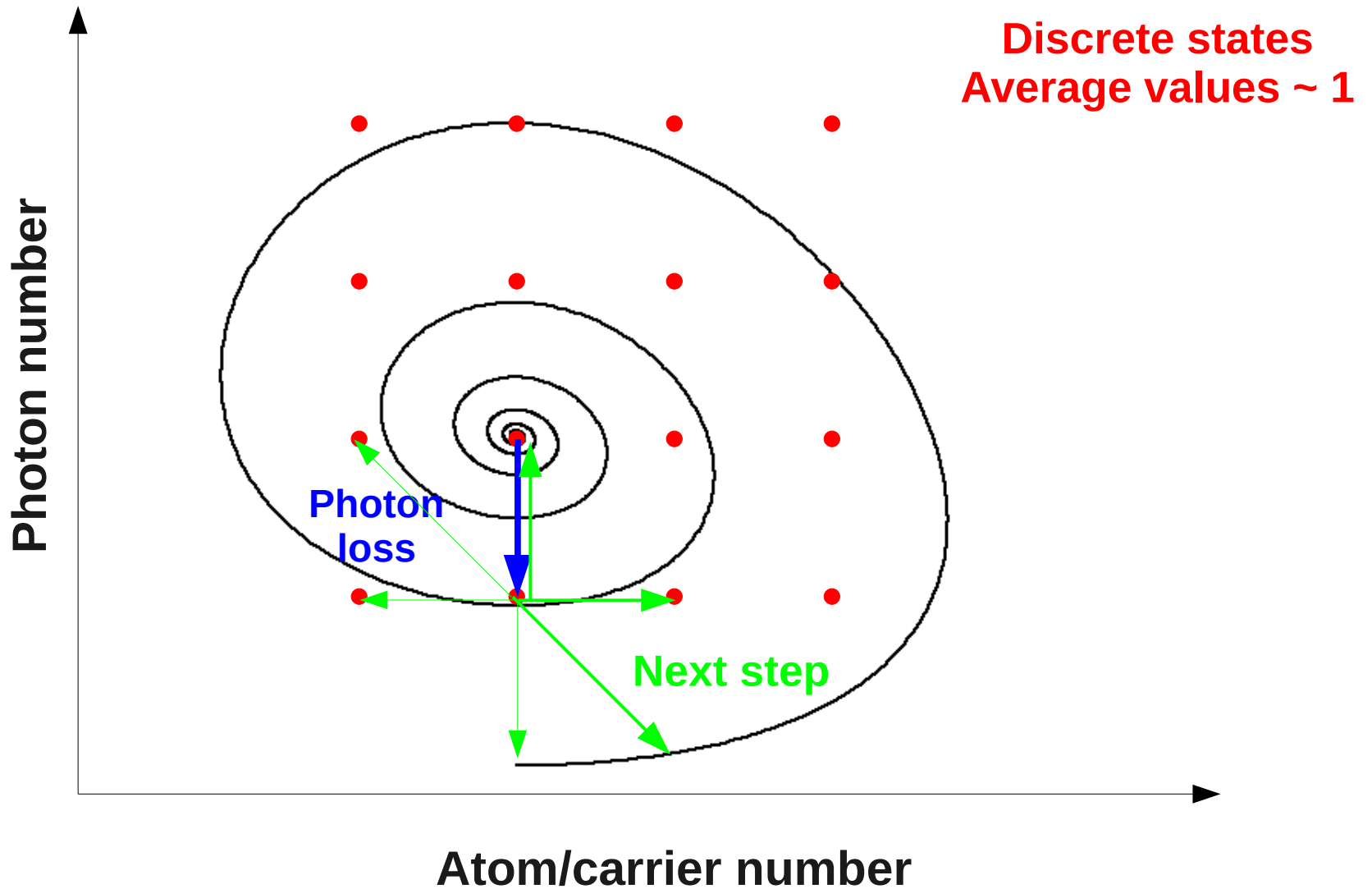
Origin of oscillations



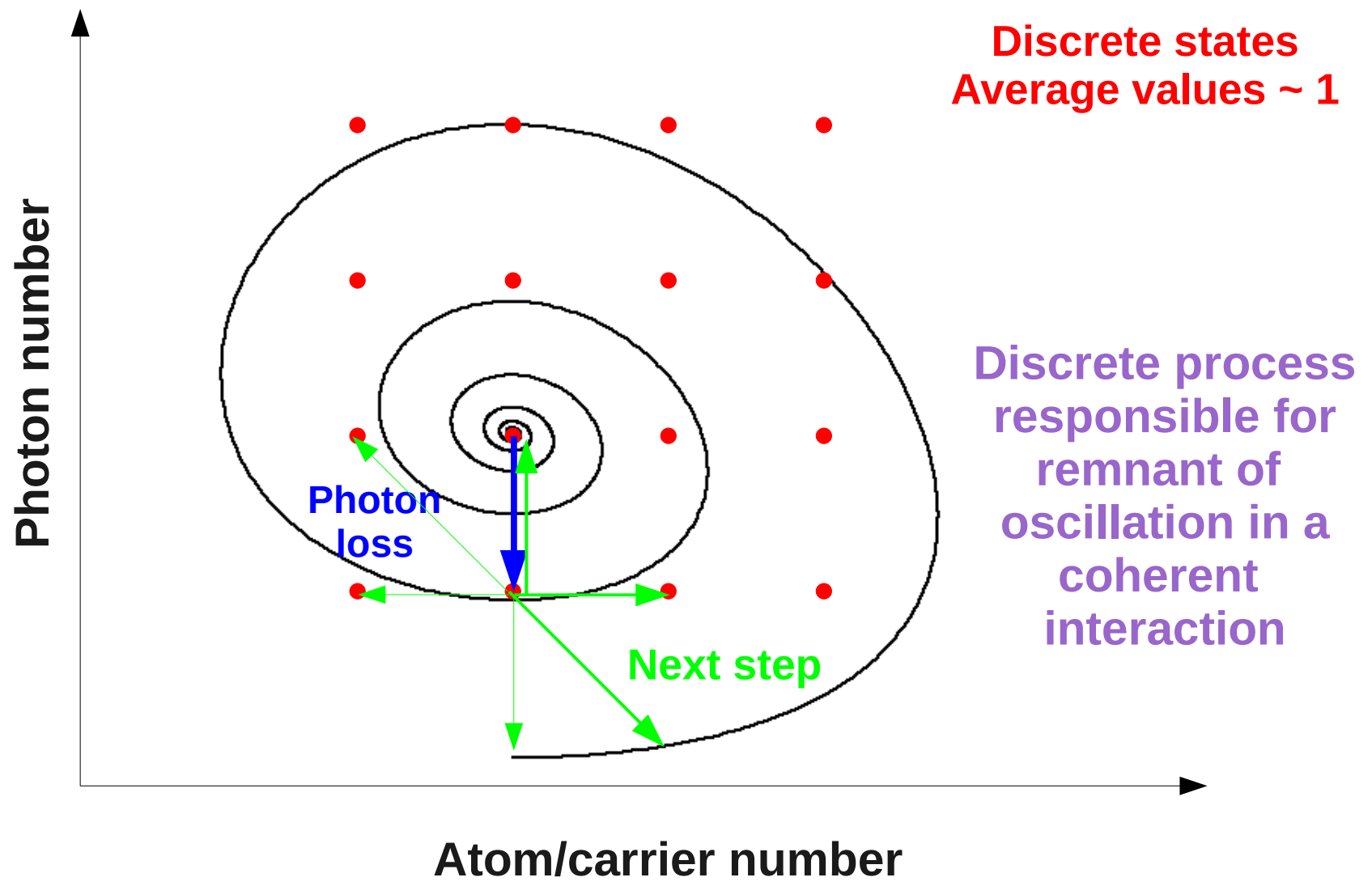
Origin of oscillations



Origin of oscillations



Origin of oscillations

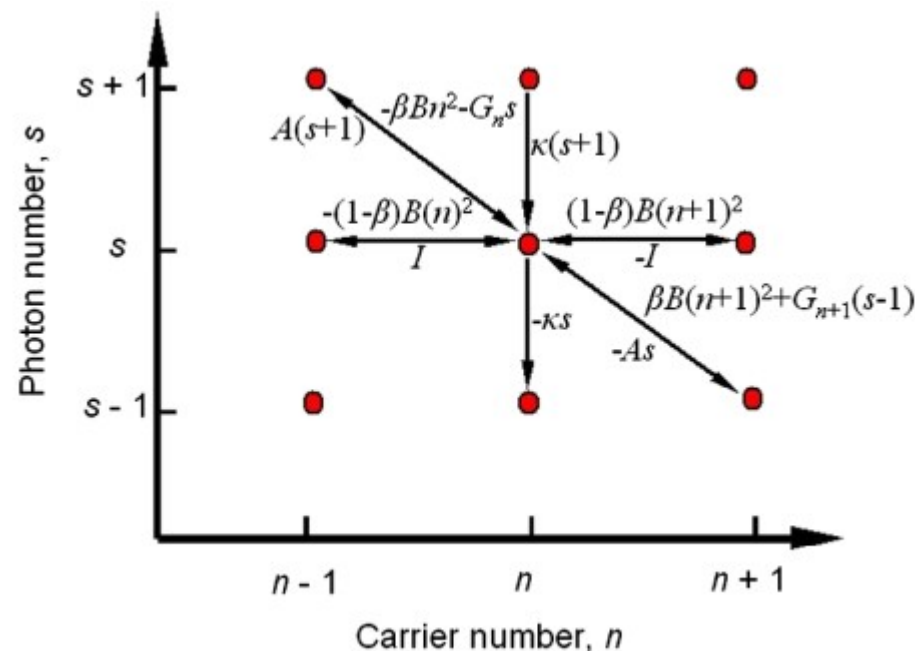


Quantum Fluctuations in Small Lasers

Kaushik Roy-Choudhury and Stephan Haas, A. F. J. Levi

Master equation approach

$$N_{eqs} = n s$$



$$\begin{aligned} \frac{dP_{n,s}}{dt} = & -\kappa(sP_{n,s} - (s+1)P_{n,s+1}) - (sG_nP_{n,s} - (s-1)G_{n+1}P_{n+1,s-1}) - (sAP_{n,s} - (s+1)AP_{n-1,s+1}) \\ & - \beta B(n^2P_{n,s} - (n+1)^2P_{n+1,s-1}) - (1-\beta)B(n^2P_{n,s} - (n+1)^2P_{n+1,s}) - \frac{I}{e}(P_{n,s} - P_{n-1,s}) \end{aligned} \quad (1)$$

Phys. Rev. Lett. **102**, 053902 (2009)

Uniform random walk
on the grid defined by
the Master Equation

Pulsing regime

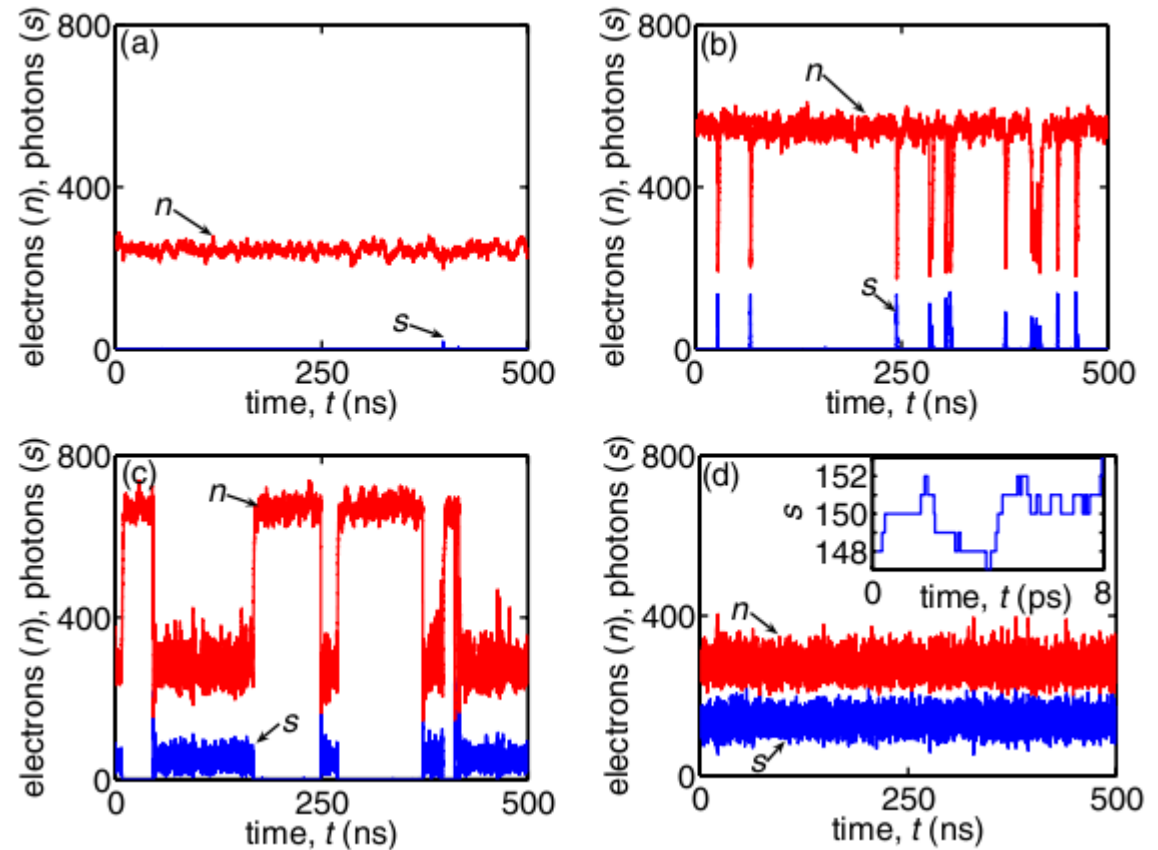
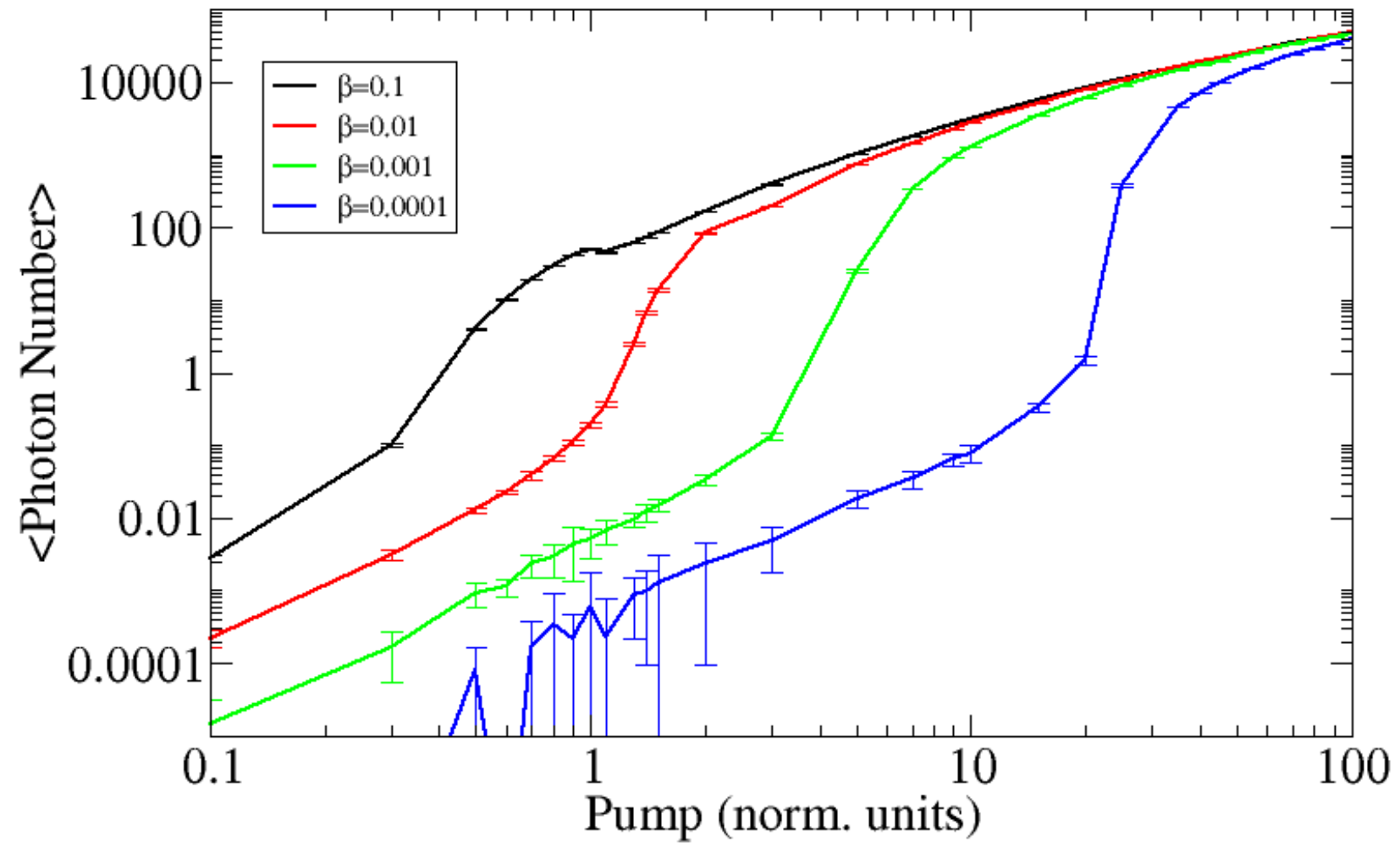


FIG. 4 (color online). Time evolution of electrons and photons calculated by the random walk method. (a) Current, $I = 9.6$ nA. (b) $I = 48$ nA. (c) $I = 72$ nA. (d) $I = 192$ nA. The inset shows discrete step changes in photon number with time. Parameters as in Fig. 2.

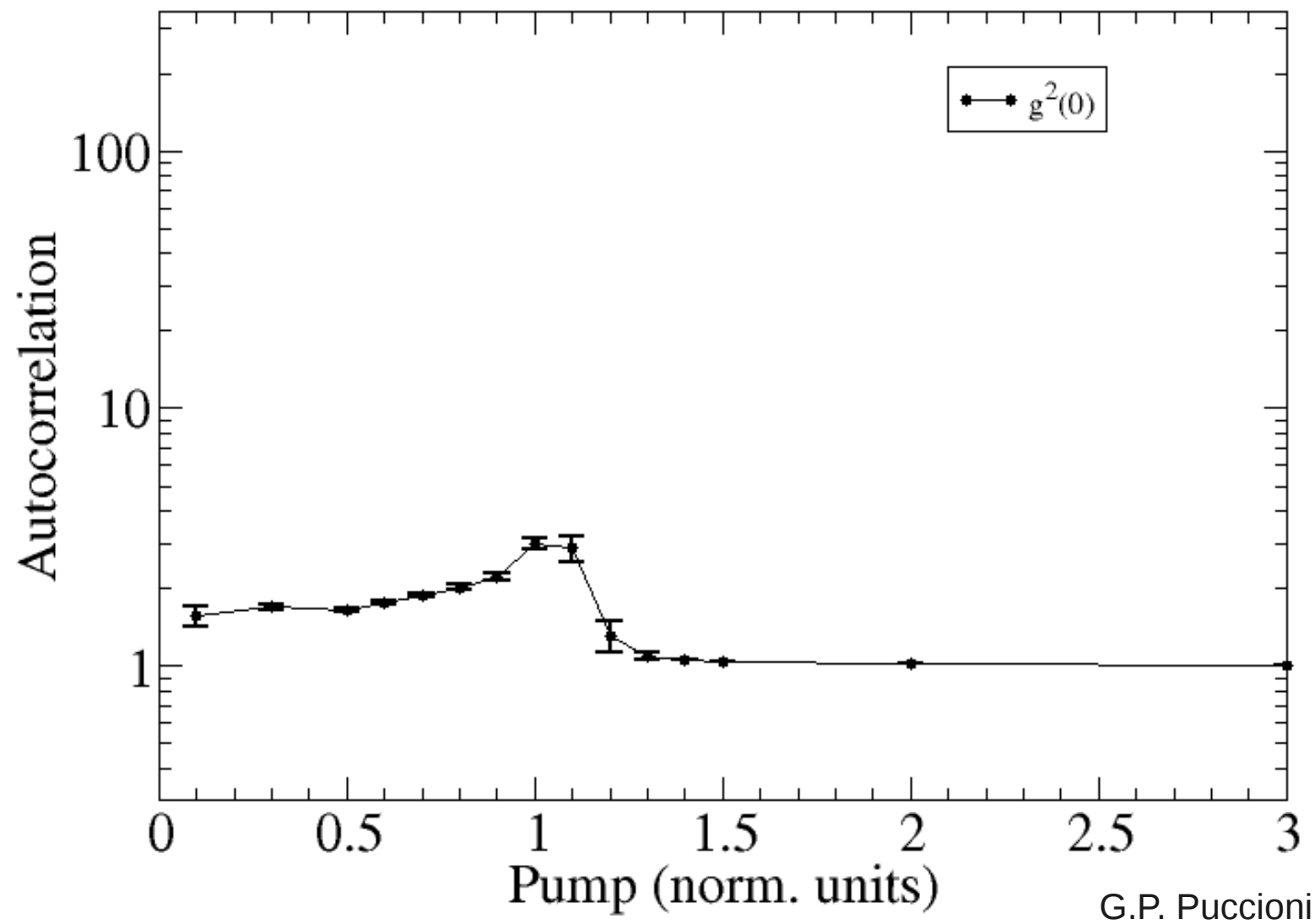
Preliminary results



G.P. Puccioni and G.L. Lippi

Preliminary results

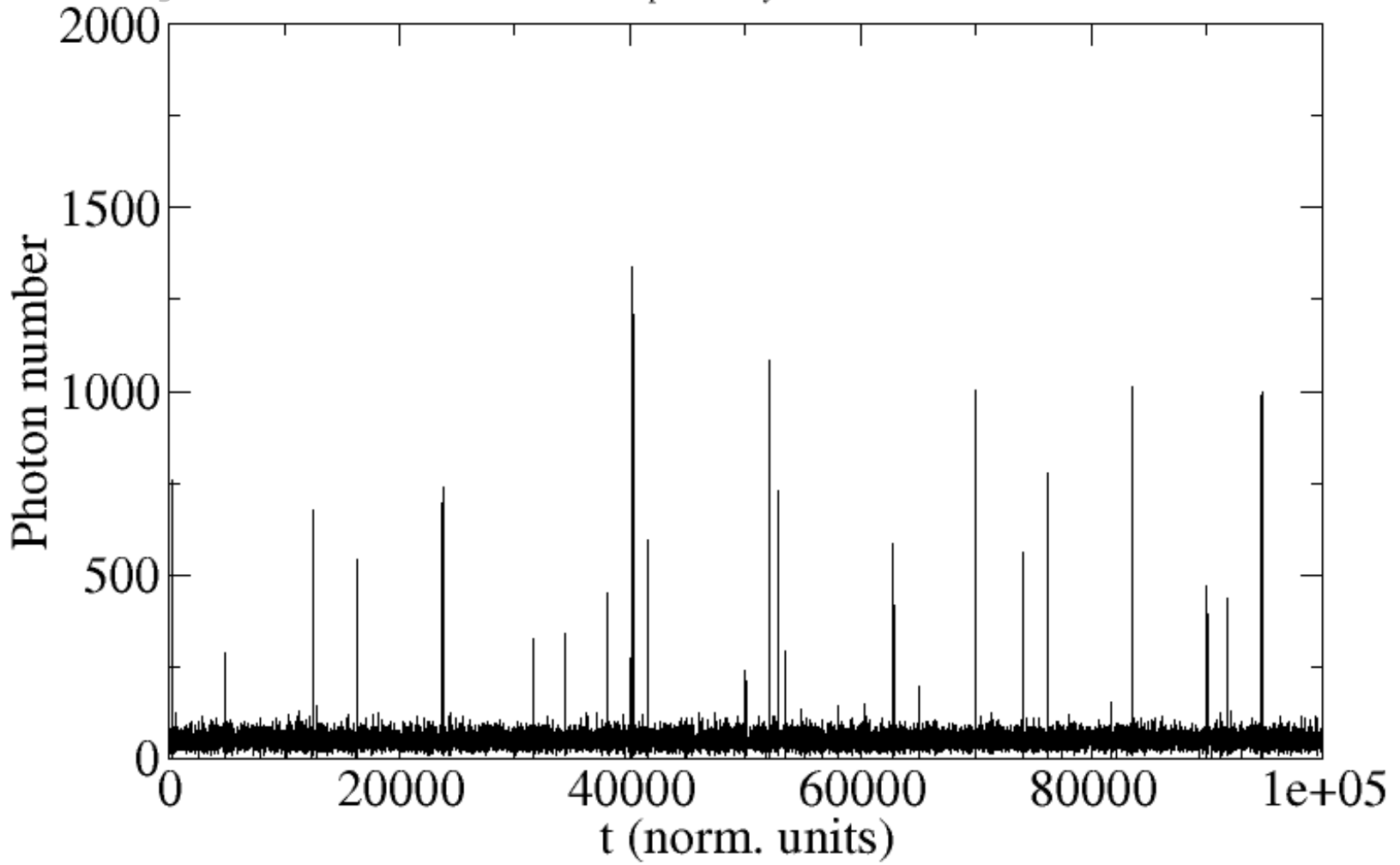
$$\beta = 0.1$$



G.P. Puccioni and G.L. Lippi

Preliminary results

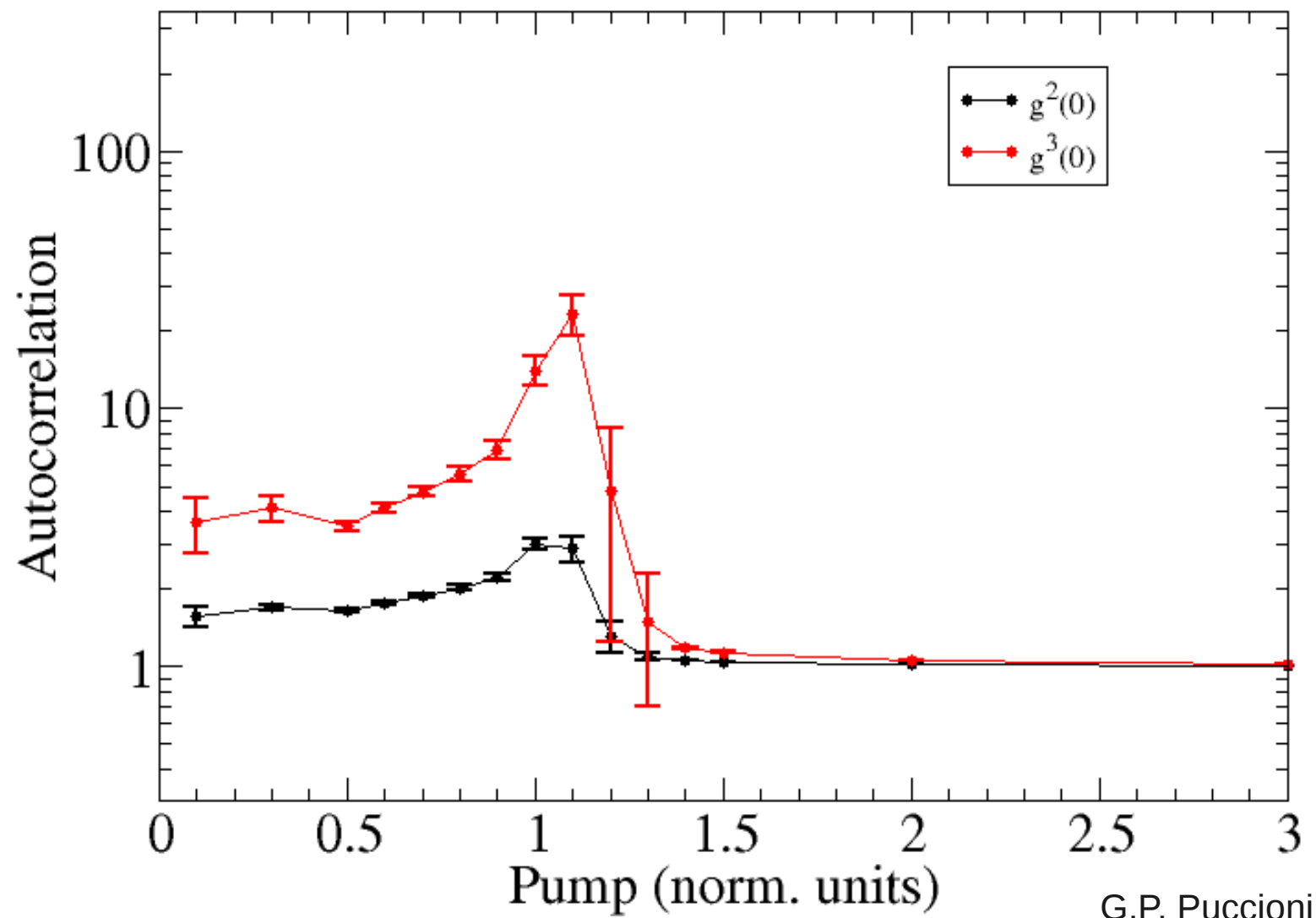
beta=0.1 p=1.2
print every 1000



G.P. Puccioni and G.L. Lippi

Preliminary results

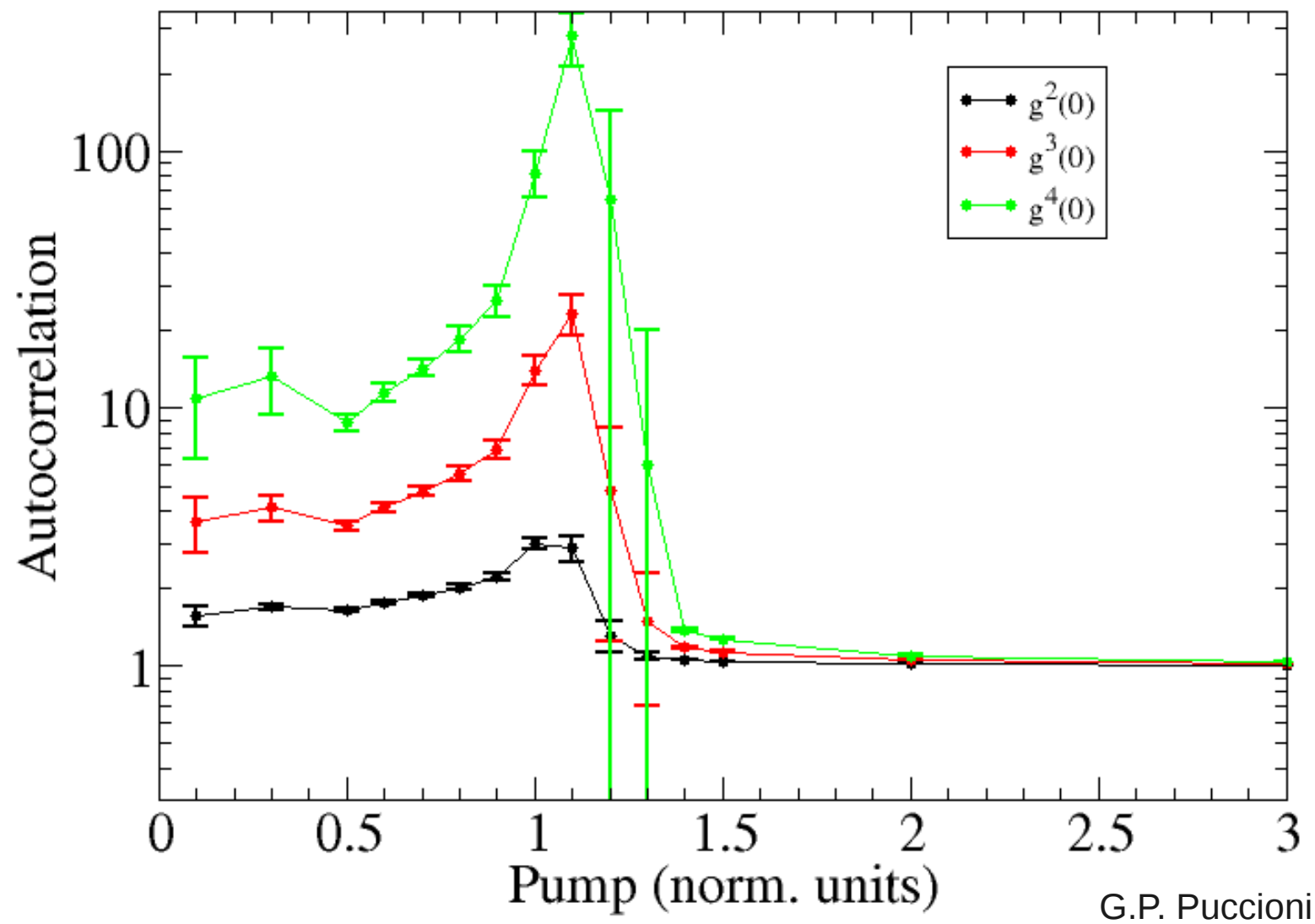
$\beta = 0.1$



G.P. Puccioni and G.L. Lippi

Preliminary results

$\beta = 0.1$



G.P. Puccioni and G.L. Lippi

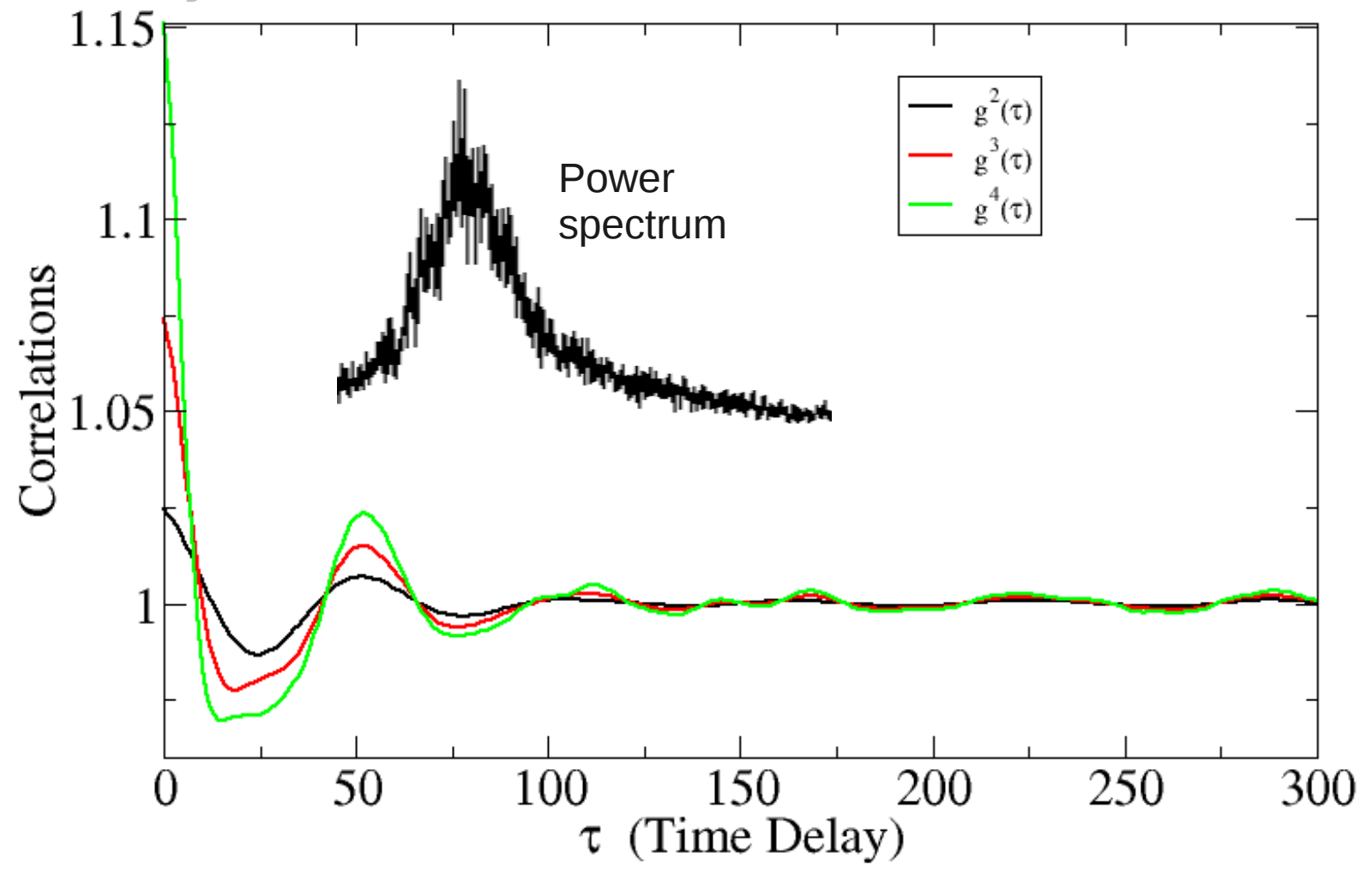
Summary

From First Principles, Granular Modeling:

- **Strong spiking regime**
- **$g^{(2)}(0)$ grows and then decreases**
- **Strong fluctuations in $g^{(2)}(0)$ before reaching coherent value**
- **$g^{(3)}(0)$ and $g^{(4)}(0)$ converge “later”**
- **Increased sensitivity to fluctuations in higher order correlations (especially $g^{(4)}(0)$)**

Preliminary results

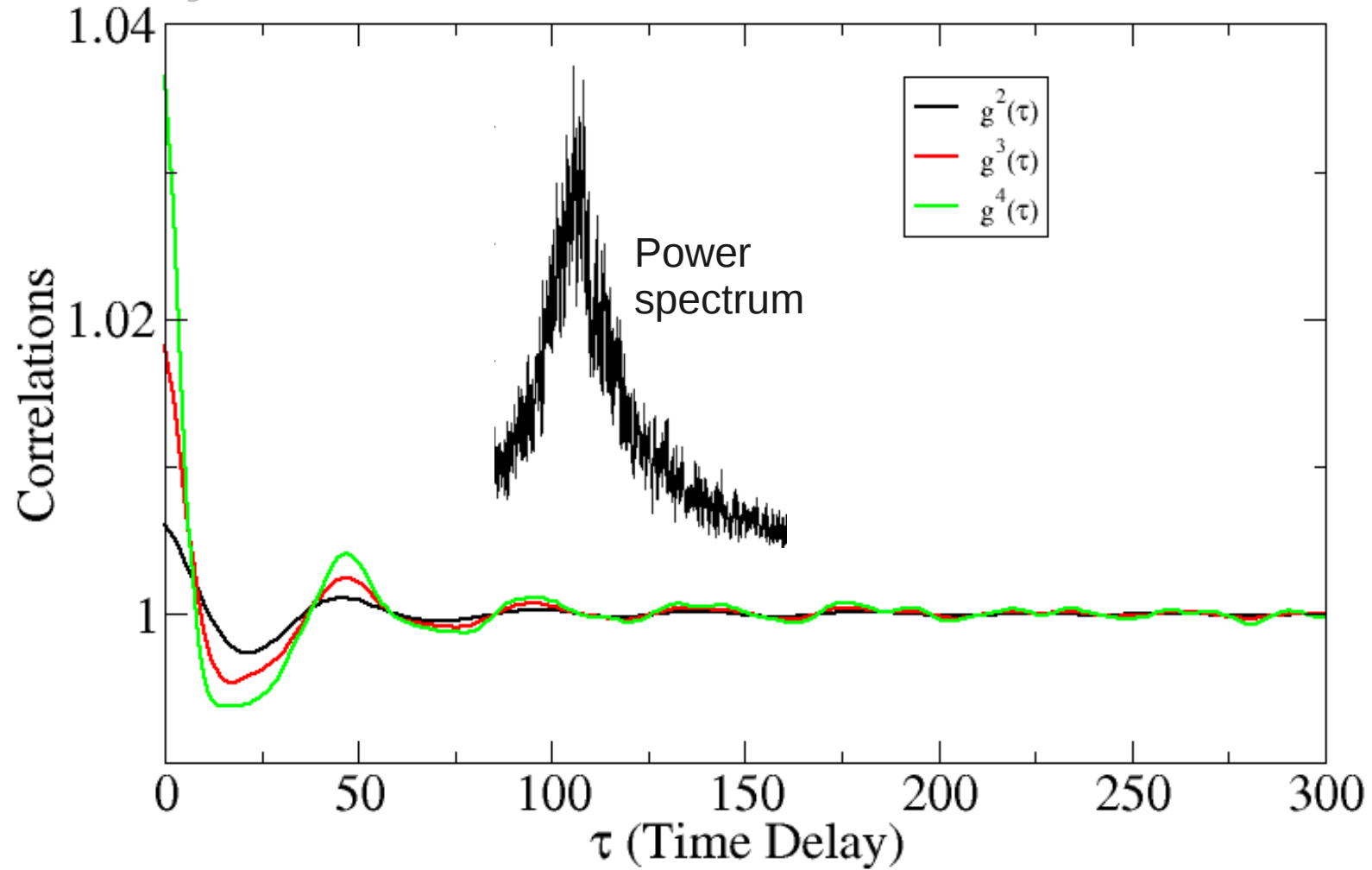
Pump=3.5 $\beta=0.01$



G.P. Puccioni and G.L. Lippi

Pump=5 $\beta=0.01$

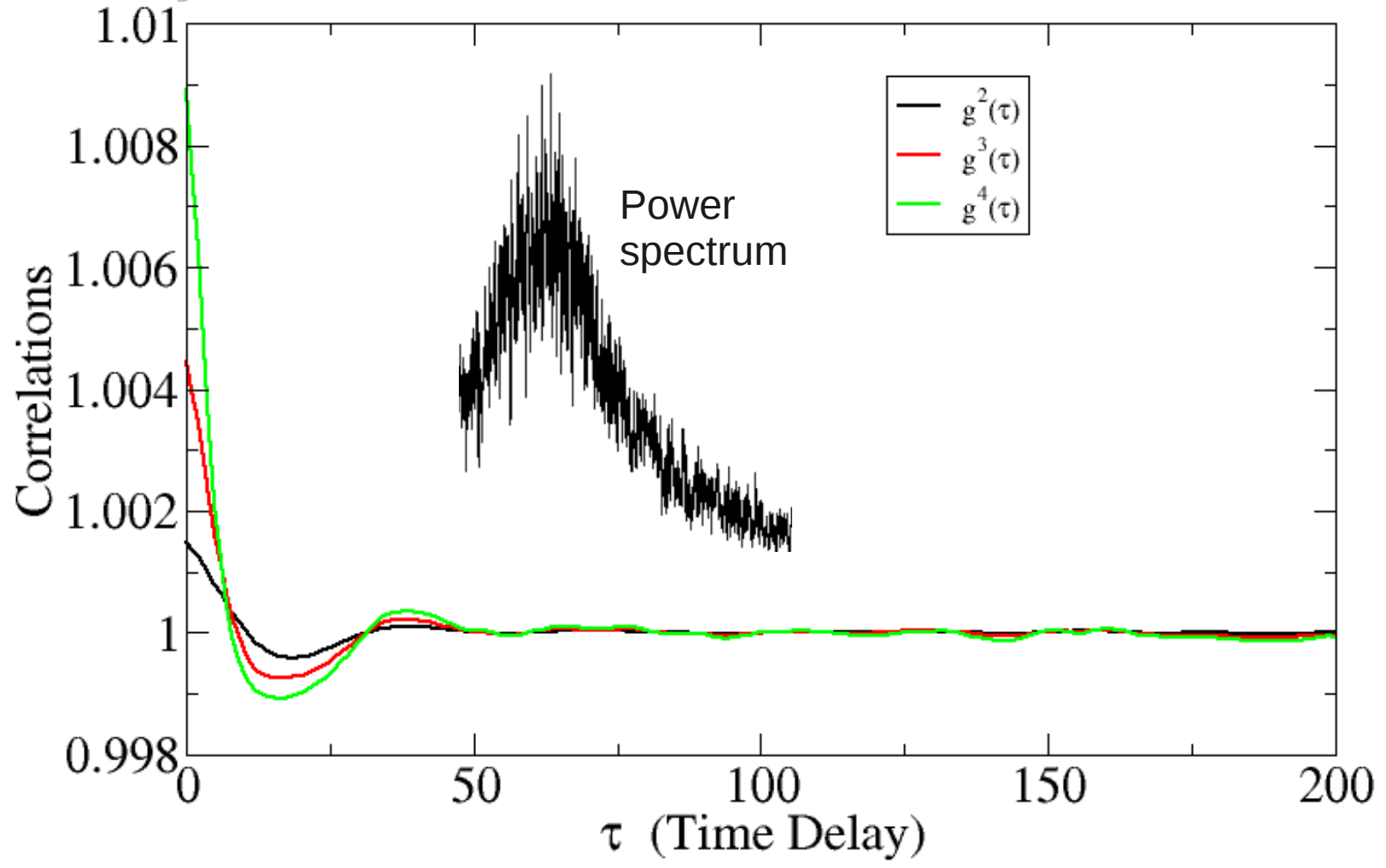
Preliminary results



G.P. Puccioni and G.L. Lippi

Preliminary results

Pump=8 $\beta=0.01$



G.P. Puccioni and G.L. Lippi

Summary

From First Principles, Granular Modeling:

- **Oscillations present in signal mimicking the physical process**
- **Power spectrum shows peak features**
- **Autocorrelation > 1 (coherent oscillations)**
- **Oscillations in correlation**
- **Higher order correlations more sensitive
(in amplitude and shape)**

Conclusions

Correlations widely used (and necessary) for characterizing coherence in micro- and nanolasers

Results strongly dependent on experimental system (reproducibility of samples, intrinsic features ...)

Most small lasers are pulsed: influence on correlations?

Problems with higher correlations

Coherent oscillations, statistical mixture of light ...

Many open questions

Thank you for your attention!

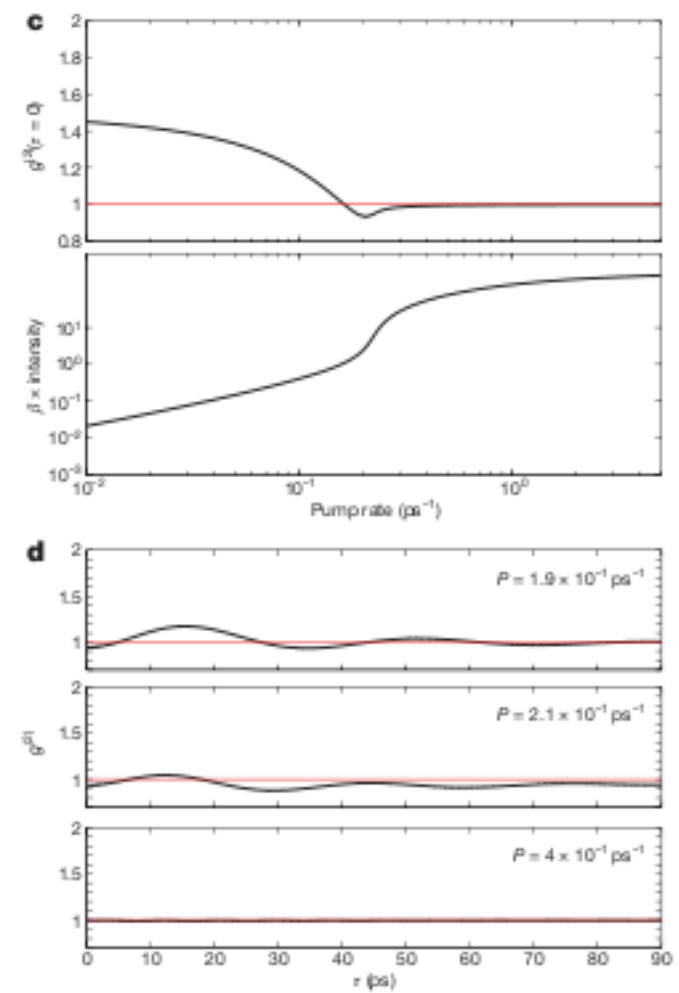
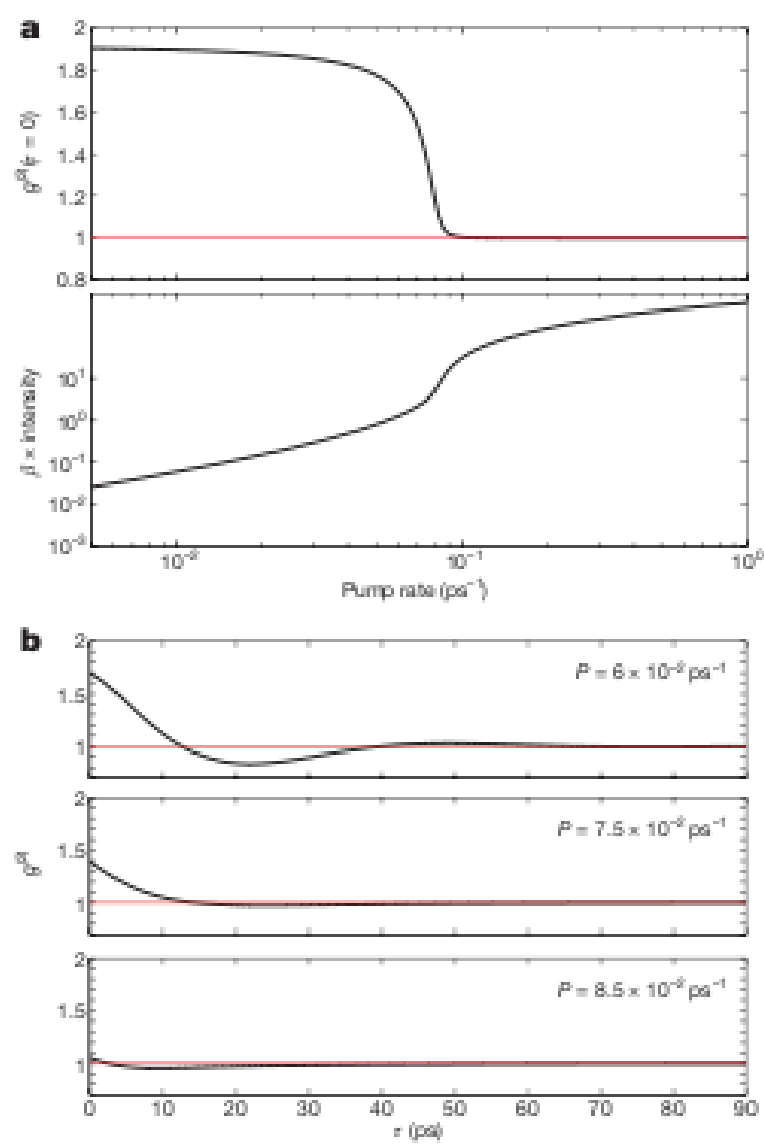
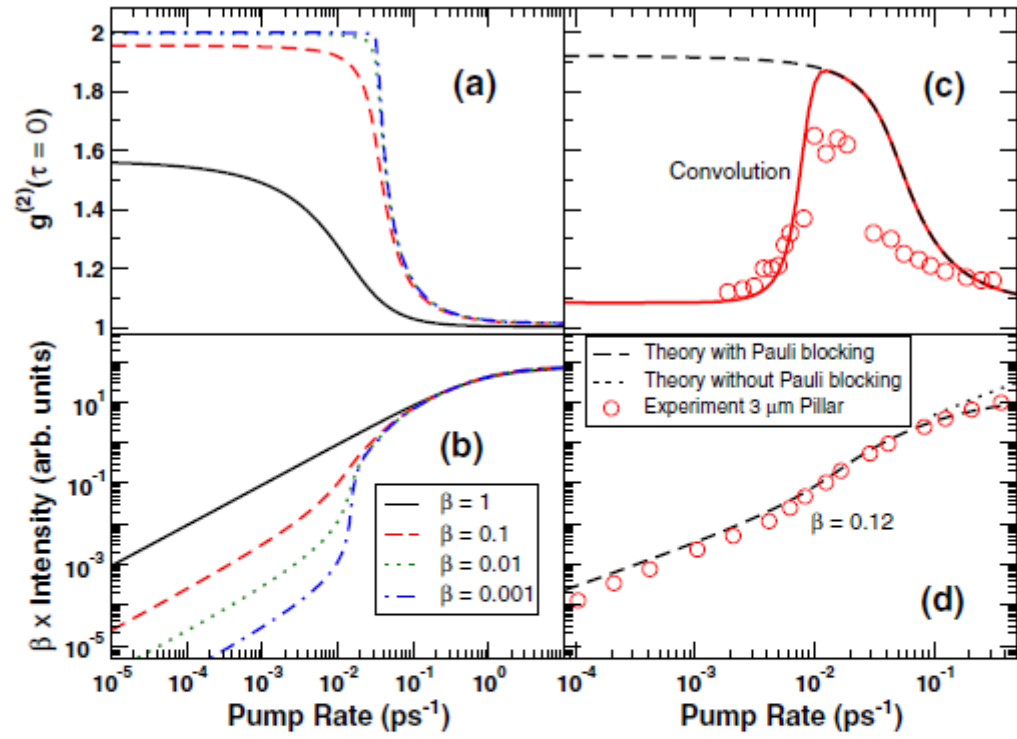


Figure 4 | Calculated zero-delay correlation functions, input-output curves and temporal dynamics of $g^{(2)}(\tau)$. **a, b**, Low-Q quantum-dot microcavity laser; **c, d**, high-Q quantum-dot microcavity laser. Selected pump rates, P , are used in **b** and **d**.

Nature **460**
Wiersig et al.



Nature **460**
Wiersig et al.

FIG. 5 (color online). (a),(b) Calculated output curves (bottom) and $g^{(2)}(0)$ (top) for various β . (c),(d) Calculated results vs experimental data (pulsed) from Fig. 3(a) for the 3 μm pillar. In (c), a convolution (solid line) with the experimental temporal resolution τ_c is shown. (d) Corresponding I/O curves, explicitly indicating the effects of pump saturation.

Higher-order photon correlations in pulsed photonic crystal nanolasers

D. Elvira,¹ X. Hachair,¹ V. B. Verma,² R. Braive,¹ G. Beaudoin,¹ I. Robert-Philip,¹ I. Sagnes,¹ B. Bæk,² S. W. Nam,²
E. A. Dauler,³ I. Abram,¹ M. J. Stevens,² and A. Beveratos^{1,4}

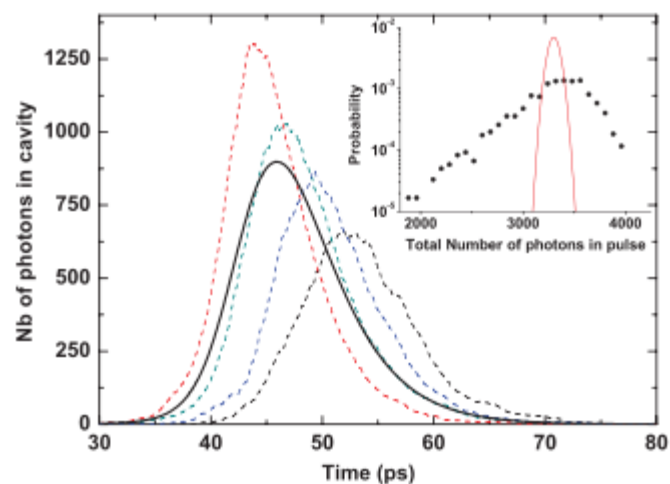


FIG. 4. (Color online) Dashed lines: Four different realizations of the stochastic rate equations at $P = 1.8P_{th}$. Solid line: The mean pulse averaged over 1500 realizations. It can be clearly seen that the longer it takes for the pulse to emerge, the smaller is its amplitude. Inset: The dots show the statistical distribution of the total number of photons per pulse at $P = 1.8P_{th}$, and the line shows the expected distribution for Poisson statistics of the same mean.

$\beta = 0.01$

